Riboflavin As Bioorthogonal Photocatalyst For The Activation Of A Pt^{IV} Prodrug

Silvia Alonso-de Castro[a], Emmanuel Ruggiero[a], Ane Ruiz-de-Angulo[a], Elixabete Rezabal[b], Juan C. Mareque-Rivas[a,c], Xabier Lopez[d], Fernando López-Gallego[a,c], Luca Salassa*[a,c,d]

[a] CIC biomaGUNE, Paseo de Miramón 182, Donostia-San Sebastián, 20014 (Spain)

[b] Farmazia Fakultatea, Kimika Fisikoa Departamentua, Euskal Herriko Unibertsitatea, UPV/EHU, Vitoria-Gasteiz, 01006 and Donostia International Physics Center (DIPC), P.K. 1072, Donostia-San Sebastián, 20080 (Spain)

[c] Ikerbasque, Basque Foundation for Science, Bilbao, 48011 (Spain)

[d] Donostia International Physics Center (DIPC), P.K. 1072, and Kimika Fakultatea, Euskal Herriko Unibertsitatea, UPV/EHU, Donostia-San Sebastián 20080 (Spain)

Electronic Supplementary Information

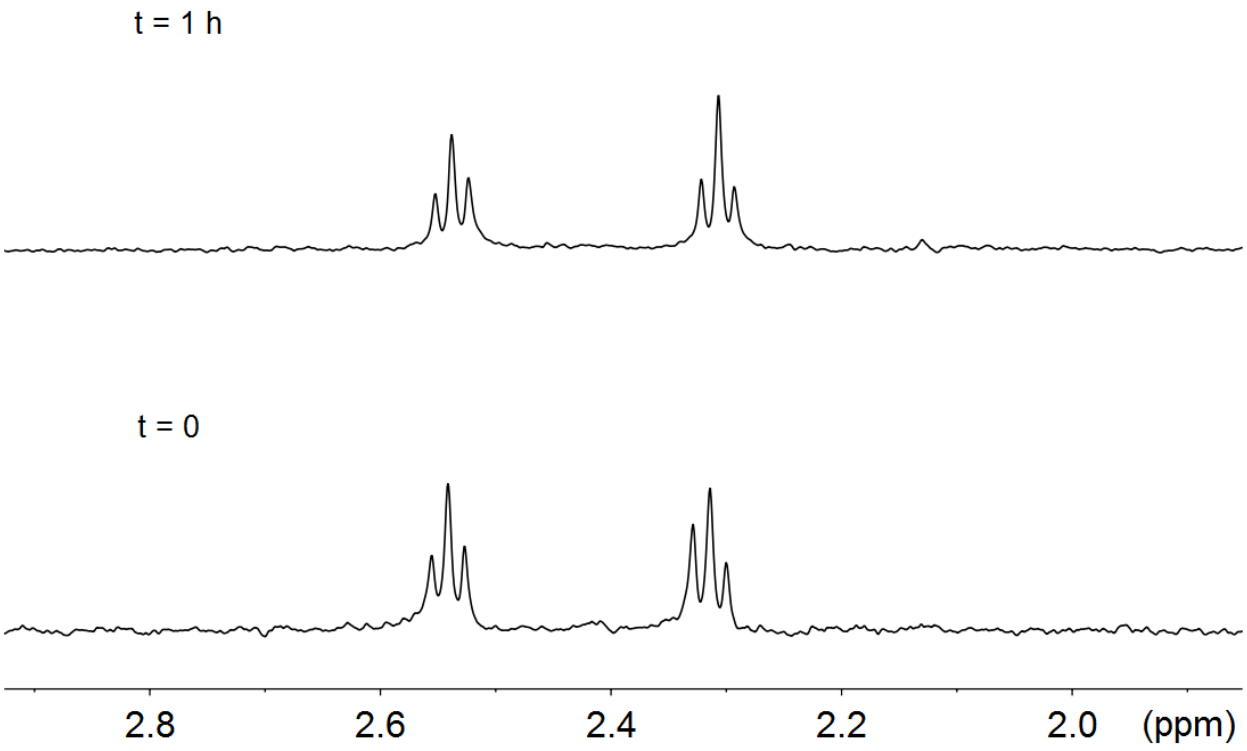

Figure S1. Photostability of **1** in H_2O (pH 6). ^1H NMR control spectra of a H_2O/D_2O solution (9:1) of **1** under 460-nm light irradiation (2.5 $mW \cdot cm^{-2}$) for 1 h.

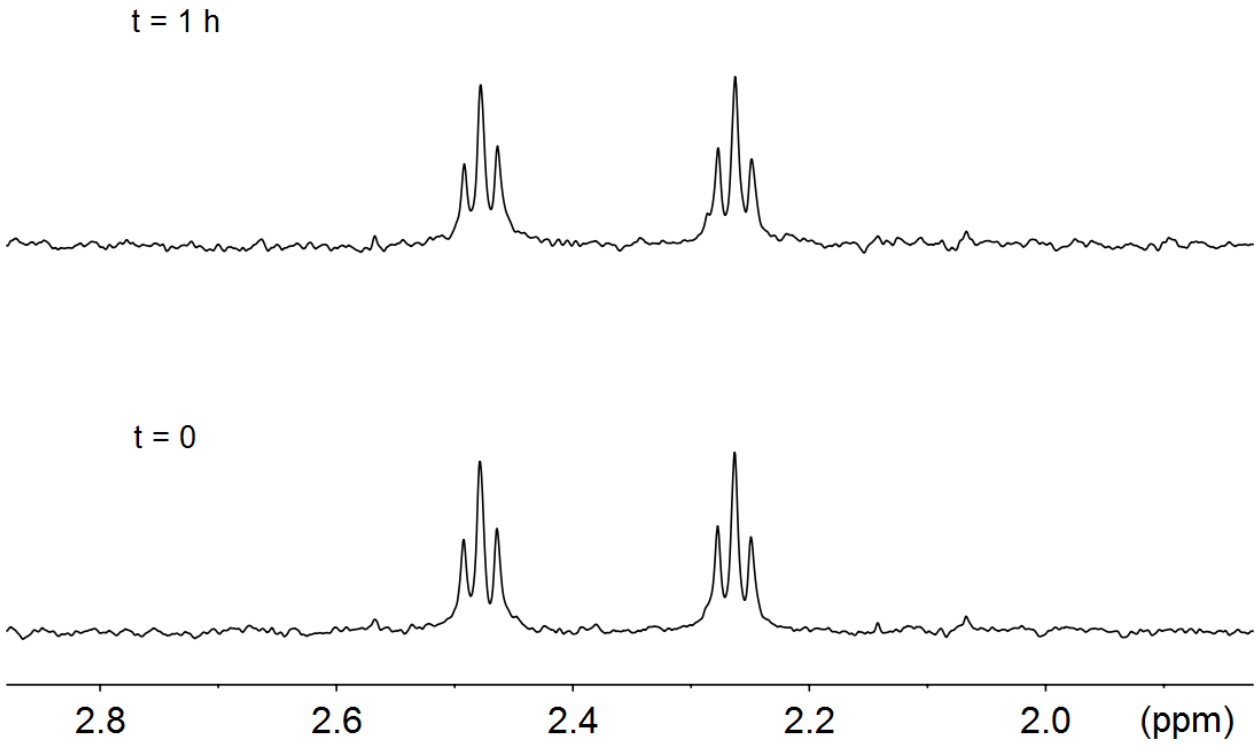

Figure S2. Photostability of **1** in phosphate buffer (PB). ^{1}H NMR control spectra of a PB/D_2O solution (9:1, PB 100 mM, pH 5.5) of **1** under 460-nm light irradiation (2.5 mW·cm^{-2}) for 1 h.

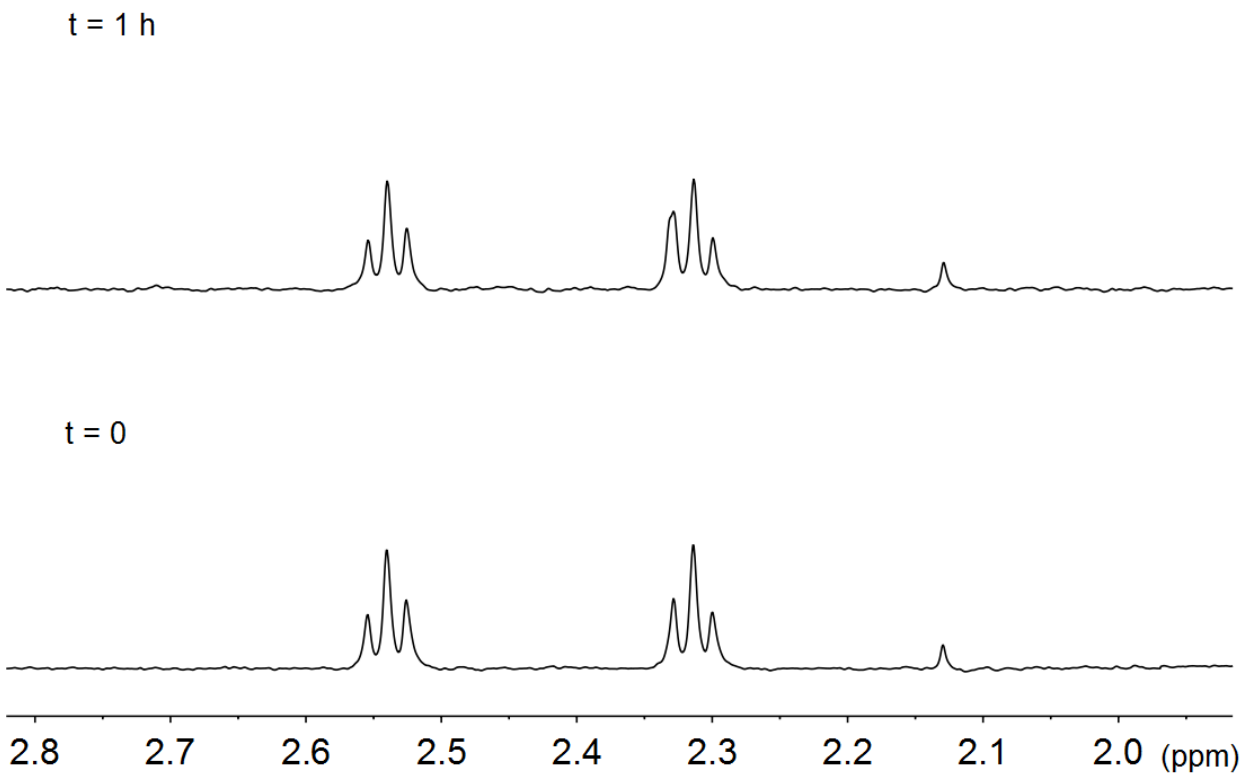

Figure S3. Photostability of **1** in MES buffer. ^{1}H NMR control spectra of a MES/D_2O solution (9:1, MES 18 mM, pH 6.0) of **1** under 460-nm light irradiation (2.5 mW·cm^{-2}) for 1 h.

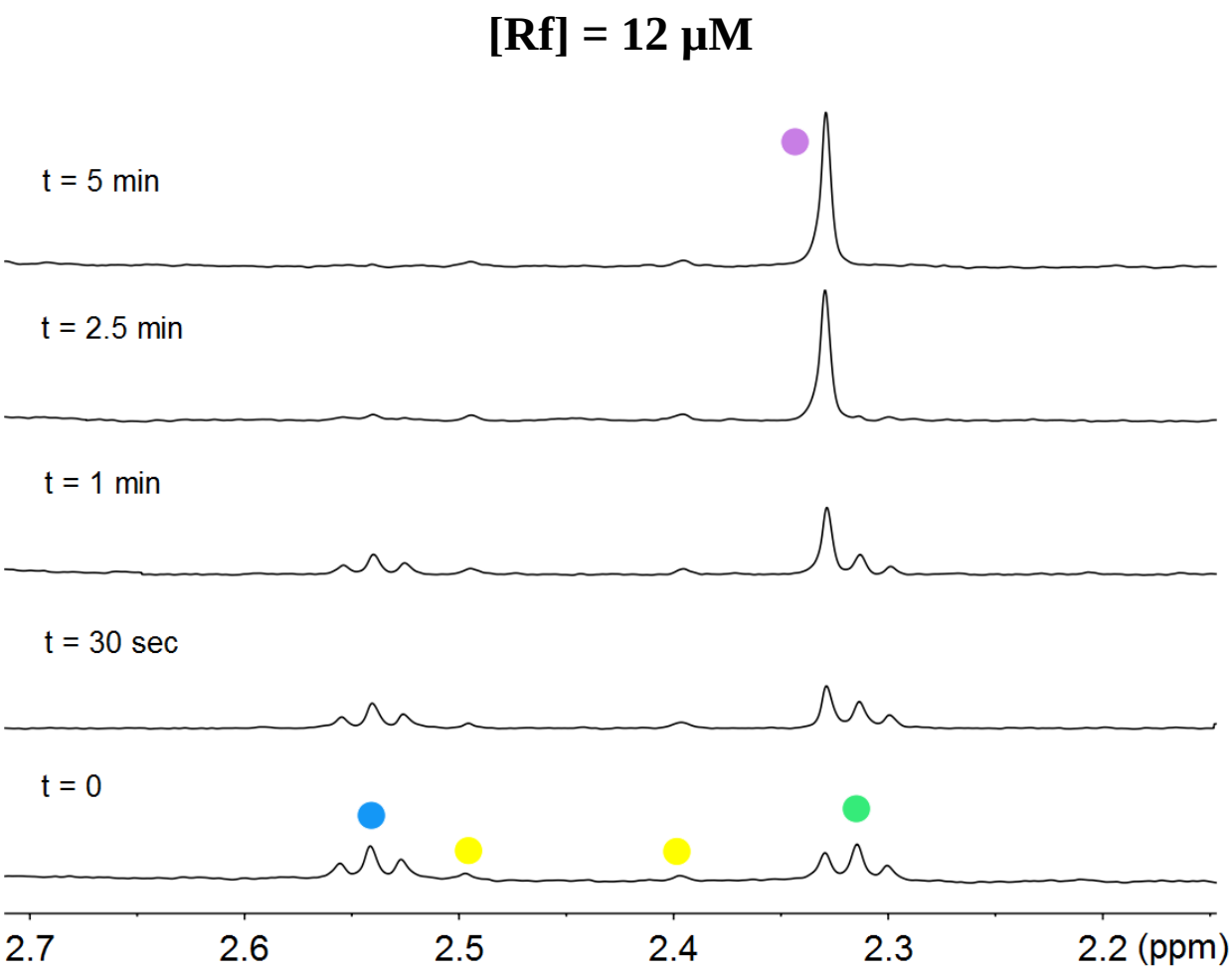

Figure S4. Photolysis of **1** in MES buffer in the presence of 12 µM **Rf**. ^{1}H NMR spectra of a MES/D_2O solution (9:1, MES 18 mM, pH 6.0) of 120 µM **1** and 12 µM **Rf** under 460-nm light irradiation (2.5 $mW \cdot cm^{-2}$) for t_{irr} = 0 sec, 30 sec, 1 min, 2.5 min and 5 min. ^{1}H NMR signal labelling: ● Pt–$OCO\mathbf{CH_2}CH_2CO_2^-$, ● Pt–$OCOCH_2\mathbf{CH_2}CO_2^-$, ● methyl groups of **Rf** isoalloxazine ring, ● free $^-O_2C\mathbf{CH_2CH_2}CO_2^-$.

[Rf] = 24 µM

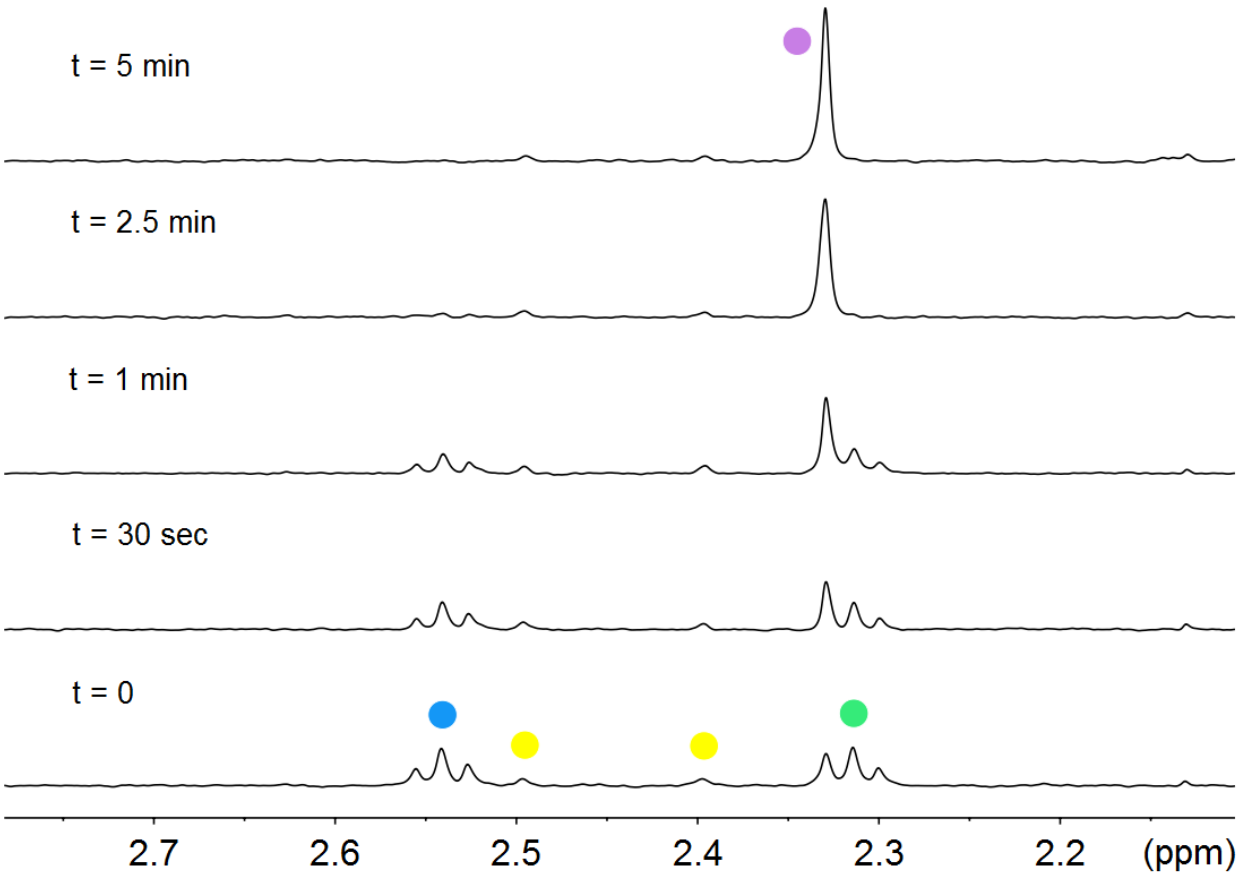

Figure S5. Photolysis of **1** in MES buffer in the presence of 24 µM **Rf**. ^{1}H NMR spectra of a MES/D_2O solution (9:1, MES 18 mM, pH 6.0) of 120 µM **1** and 24 µM **Rf** under 460-nm light irradiation (2.5 $mW \cdot cm^{-2}$) for t_{irr} = 0 sec, 30 sec, 1 min, 2.5 min and 5 min. ^{1}H NMR signal labelling: ● Pt–OCO**CH_2**$CH_2CO_2^-$, ● Pt–OCOCH_2**CH_2**CO_2^-, ● methyl groups of **Rf** isoalloxazine ring, ● free ^-O_2C**CH_2CH_2**CO_2^-.

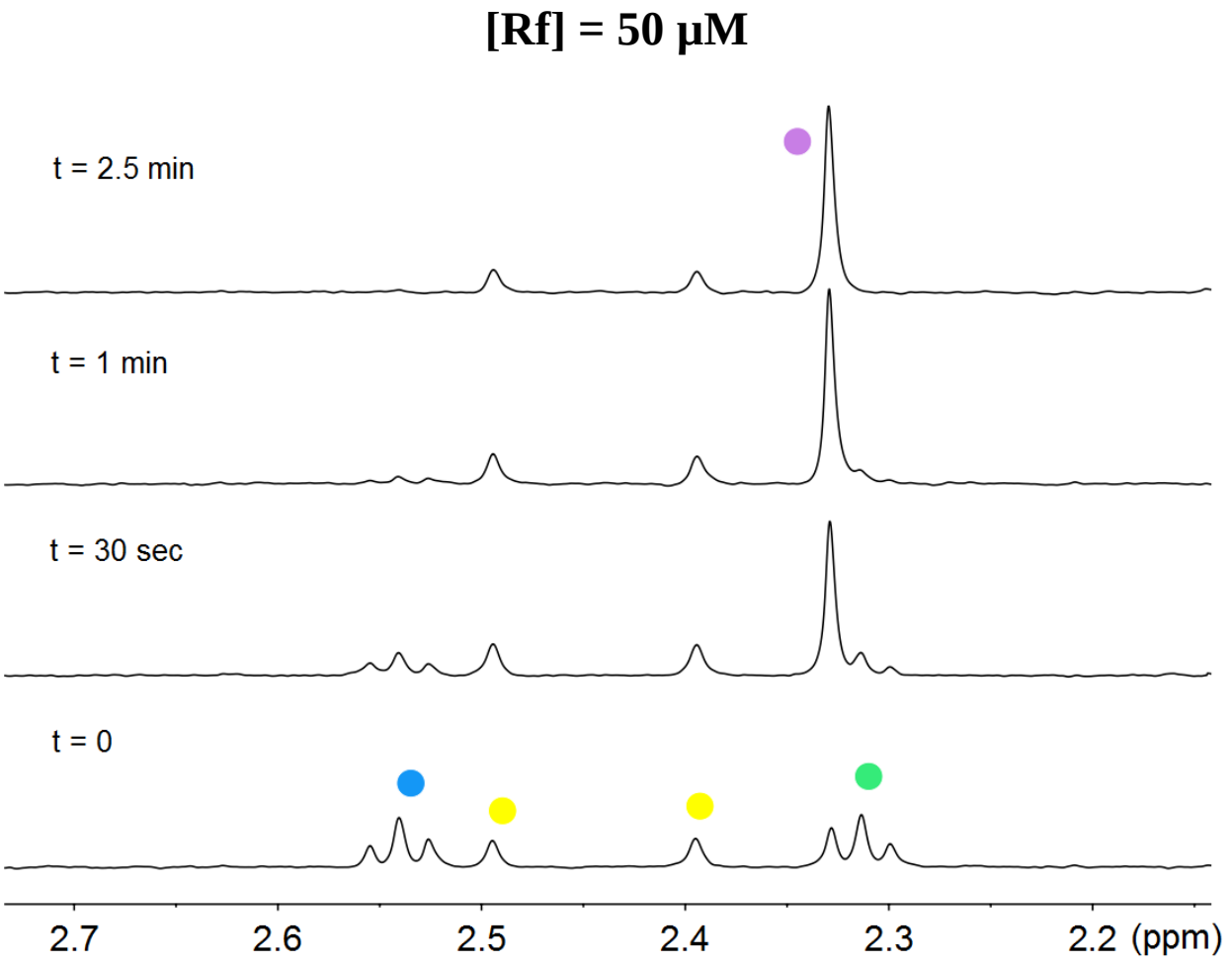

Figure S6. Photolysis of **1** in MES buffer in the presence of 50 µM **Rf**. ^{1}H NMR spectra of a MES/D_2O solution (9:1, MES 18 mM, pH 6.0) of 120 µM **1** and 50 µM **Rf** under 460-nm light irradiation (2.5 $mW \cdot cm^{-2}$) for t_{irr} = 0 sec, 30 sec, 1 min and 2.5 min. ^{1}H NMR signal labelling: ● Pt–OCO**CH_2**$CH_2CO_2^-$, ● Pt–OCOCH_2**CH_2**CO_2^-, ● methyl groups of **Rf** isoalloxazine ring, ● free ^-O_2C**CH_2CH_2**CO_2^-.

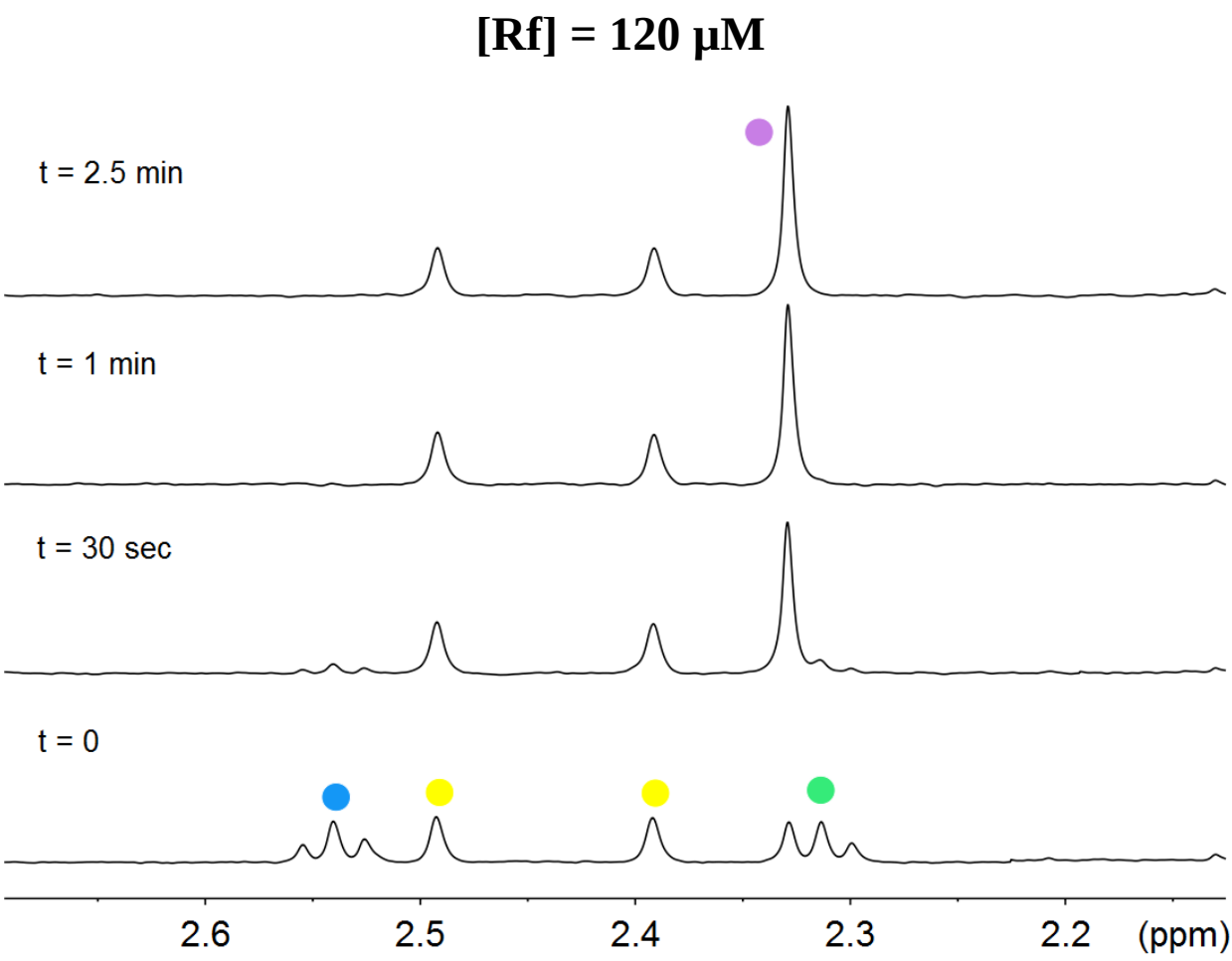

Figure S7. Photolysis of **1** in MES buffer in the presence of 120 µM **Rf**. ^{1}H NMR spectra of a MES/D_2O solution (9:1, MES 18 mM, pH = 6.0) of 120 µM **1** and 120 µM **Rf** under 460-nm light irradiation (2.5 $mW \cdot cm^{-2}$) for t_{irr} = 0 sec, 30 sec, 1 min and 2.5 min. ^{1}H NMR signal labelling: ● Pt–OCO**CH_2**$CH_2CO_2^-$, ● Pt–OCOCH_2**CH_2**CO_2^-, ● methyl groups of **Rf** isoalloxazine ring, ● free ^-O_2C**CH_2CH_2**CO_2^-.

[Rf] = 0.13 µM

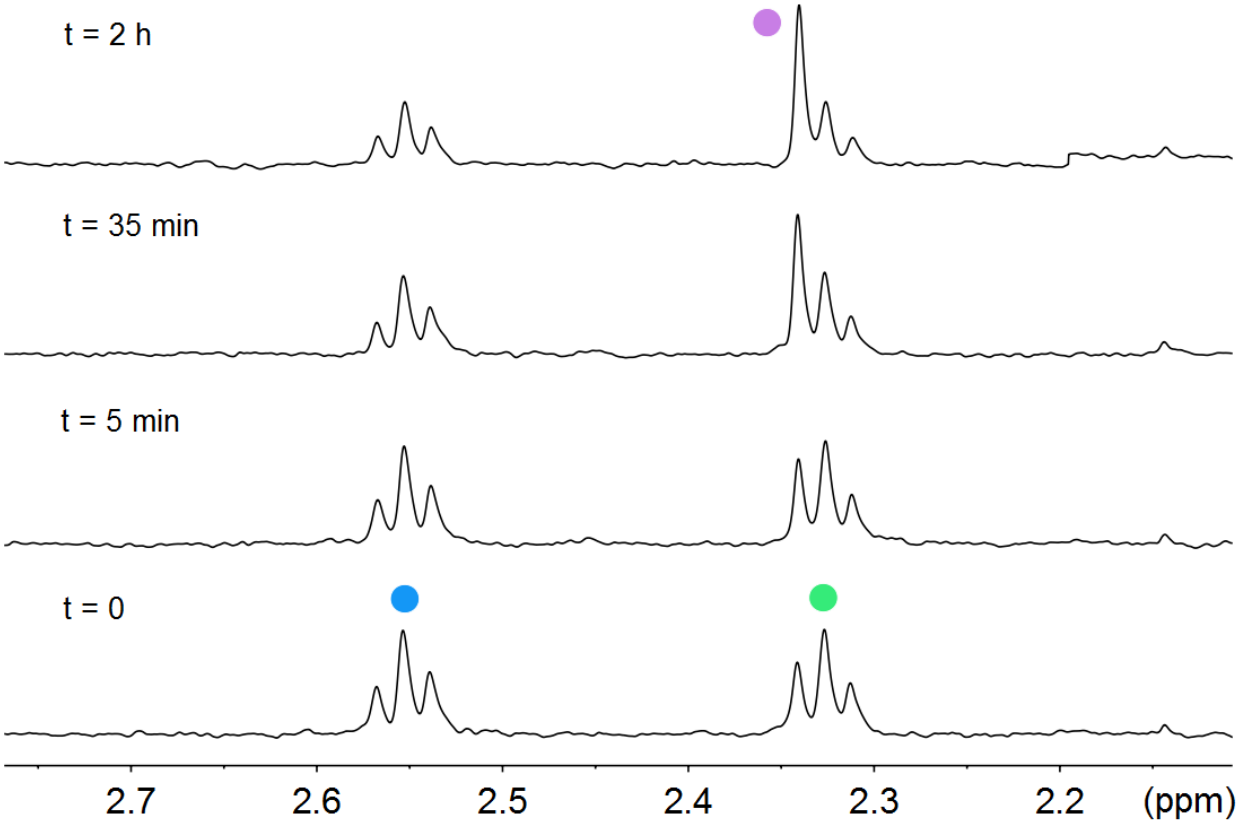

Figure S8. Photolysis of **1** in MES buffer in the presence of 0.13 µM **Rf**. ^{1}H NMR spectra of a MES/D_2O solution (9:1, MES 18 mM, pH 6.0) of 120 µM **1** and 0.13 µM **Rf** under 460-nm light irradiation (2.5 mW·cm^{-2}) for t_{irr} = 0, 5, 35 and 120 min. ^{1}H NMR signal labelling: ● Pt–OCO**C**$\mathbf{H_2}$$CH_2CO_2^-$, ● Pt–$OCOCH_2$**C**$\mathbf{H_2}$$CO_2^-$, ● free ^-O_2C**C**$\mathbf{H_2}$**C**$\mathbf{H_2}$$CO_2^-$. Methyl groups of **Rf** isoalloxazine ring are not detectable by NMR at this concentration.

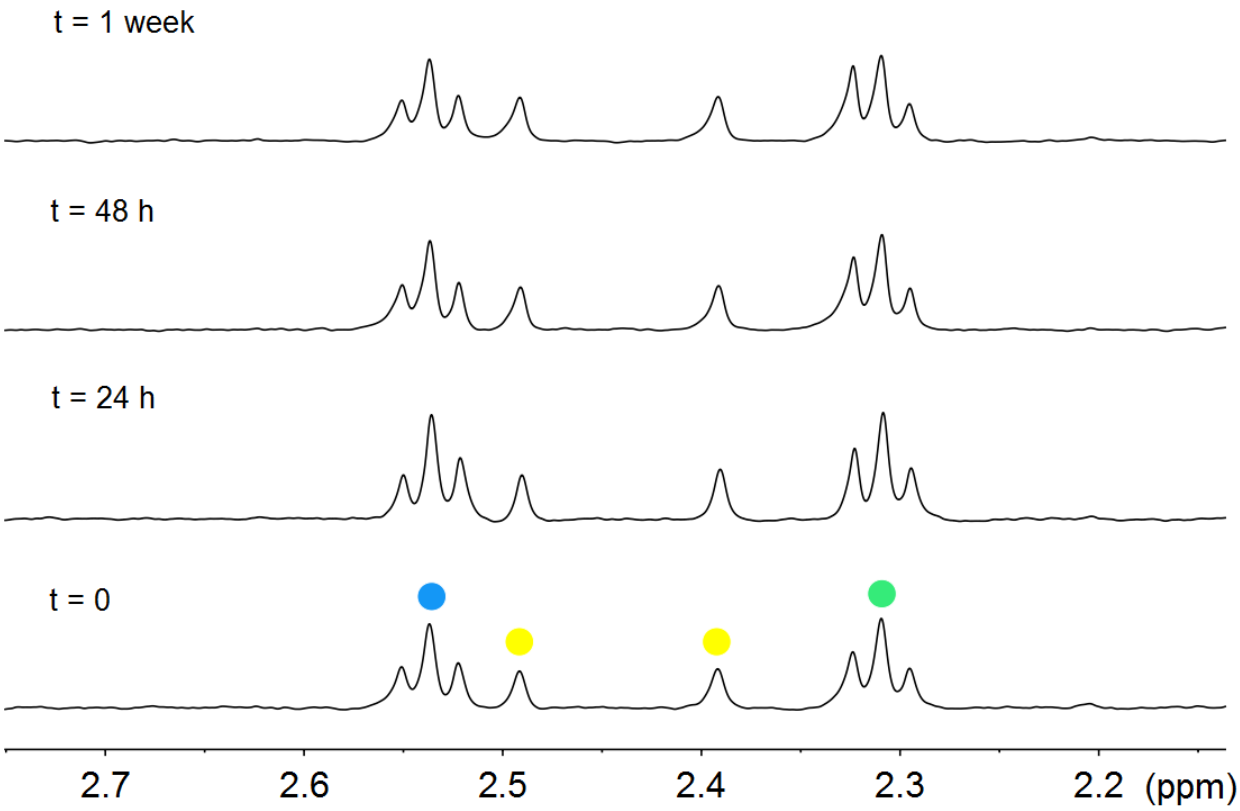

Figure S9. Stability control in the dark for **Rf/1** in MES buffer. ^{1}H NMR spectra of MES/D_2O solution (9:1, MES 18 mM, pH 6.0) containing 120 µM **1** and 50 µM **Rf** in the dark for t = 0, 24 h, 48 h and 1 week. ^{1}H NMR signal labelling: ● Pt–OCO**CH$_2$**CH$_2$CO$_2^-$, ● Pt–OCOCH$_2$**CH$_2$**CO$_2^-$ and ● methyl groups of **Rf** isoalloxazine ring.

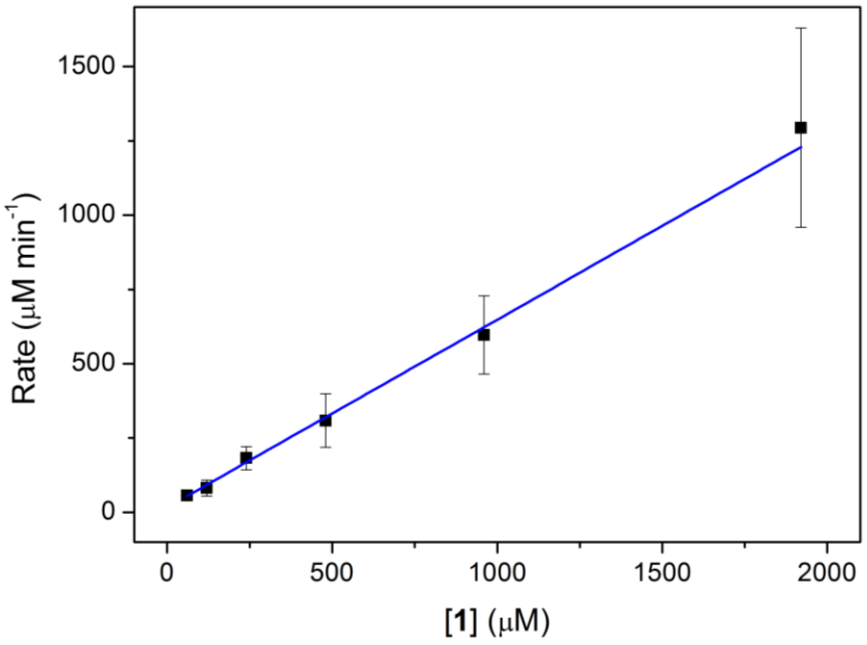

Figure S10. Dependency of photocatalytic rate on substrate (**1**). Study of the photocatalytic activation of **1** at increasing substrate concentrations ([**1**] = 60, 120, 240, 480, 960 and 1920 μM) and fixed concentrations of **Rf** (50 μM) and MES (18 mM). An irradiation time of 30 sec was used for all the samples (λ_{exc} = 460 nm, 2.5 mW·cm^{-2}).

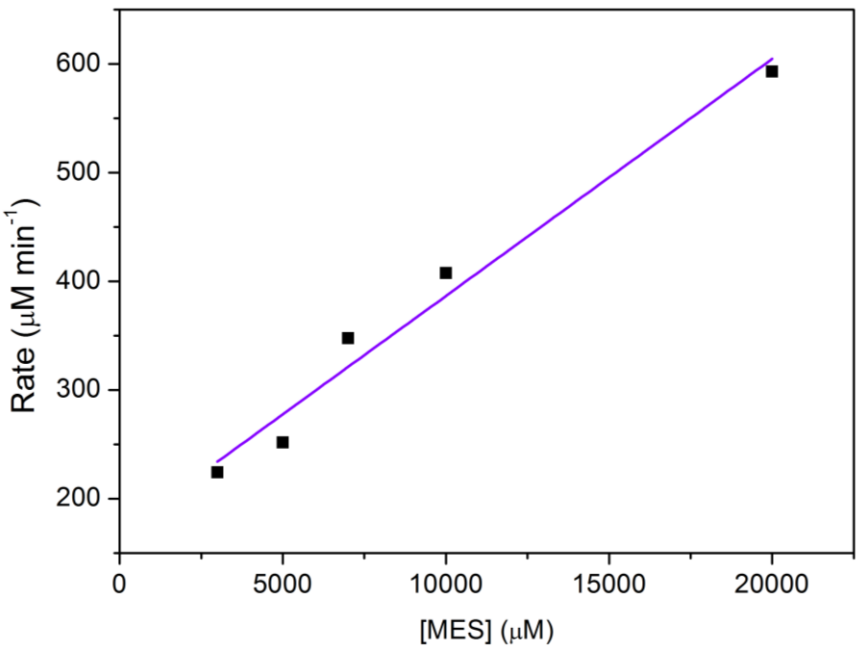

Figure S11. Dependency of photocatalytic rate on MES concentration. Photocatalytic activation of **1** at increasing concentrations of MES ([MES] = 3, 5, 7, 10, and 20 mM) and at a fixed concentration of **Rf** (50 μM) and **1** (500 μM). An irradiation time of 30 sec was set for all the samples (λ_{exc} = 460 nm, 2.5 $mW \cdot cm^{-2}$).

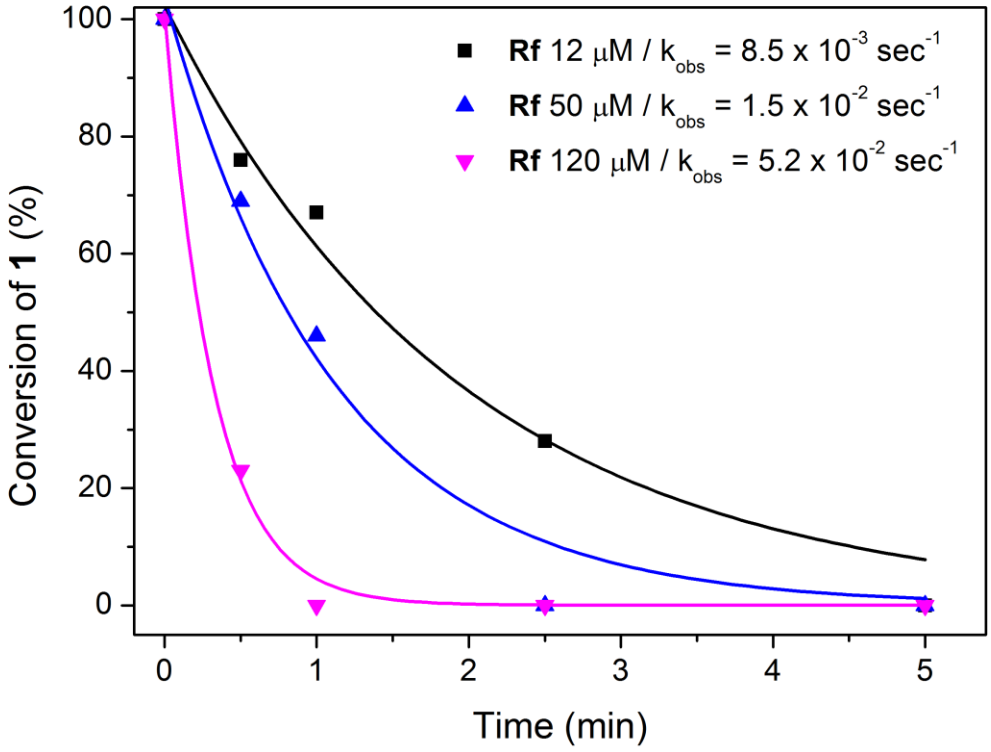

Figure S12. Dependency of photocatalytic rate on **Rf** concentration. Study of the photocatalytic activation of **1** at three different concentrations of **Rf** (12, 50 and 120 μM) and at fixed concentrations of **1** (120 μM) and MES (18 mM). The different colours lines corresponds to the fitting of the corresponding experimental data to the pseudo-first order equation $[1] = [1]_0 e^{-k_{obs}t}$, where t = time and k_{obs} = observed kinetic constant defined as $k_{obs} = k[\text{MES}]$ where k = constant of the second order reaction.

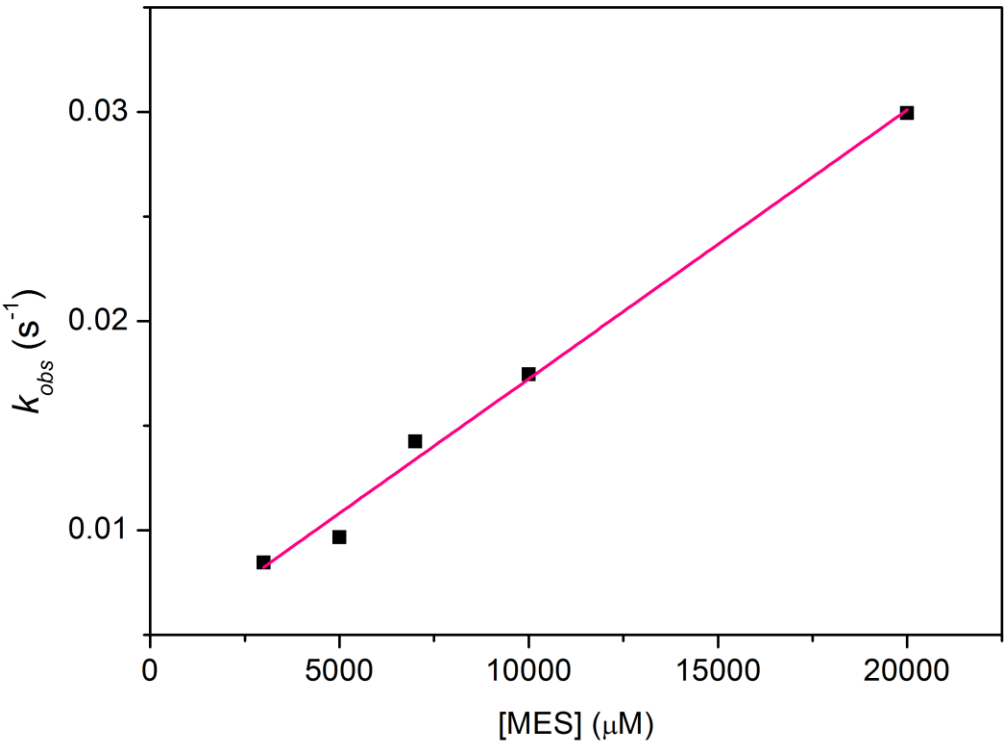

Figure S13. Dependency of photocatalytic rate constant k_{obs} on MES concentration. Study of the photocatalytic activation of **1** at increasing concentrations of MES ([MES] = 3, 5, 7, 10, and 20 mM) and at a fixed concentration of **Rf** (50 μM) and **1** (500 μM). An irradiation time of 30 sec was set for all samples (λ_{exc} = 460 nm, 2.5 mW·cm^{-2}).

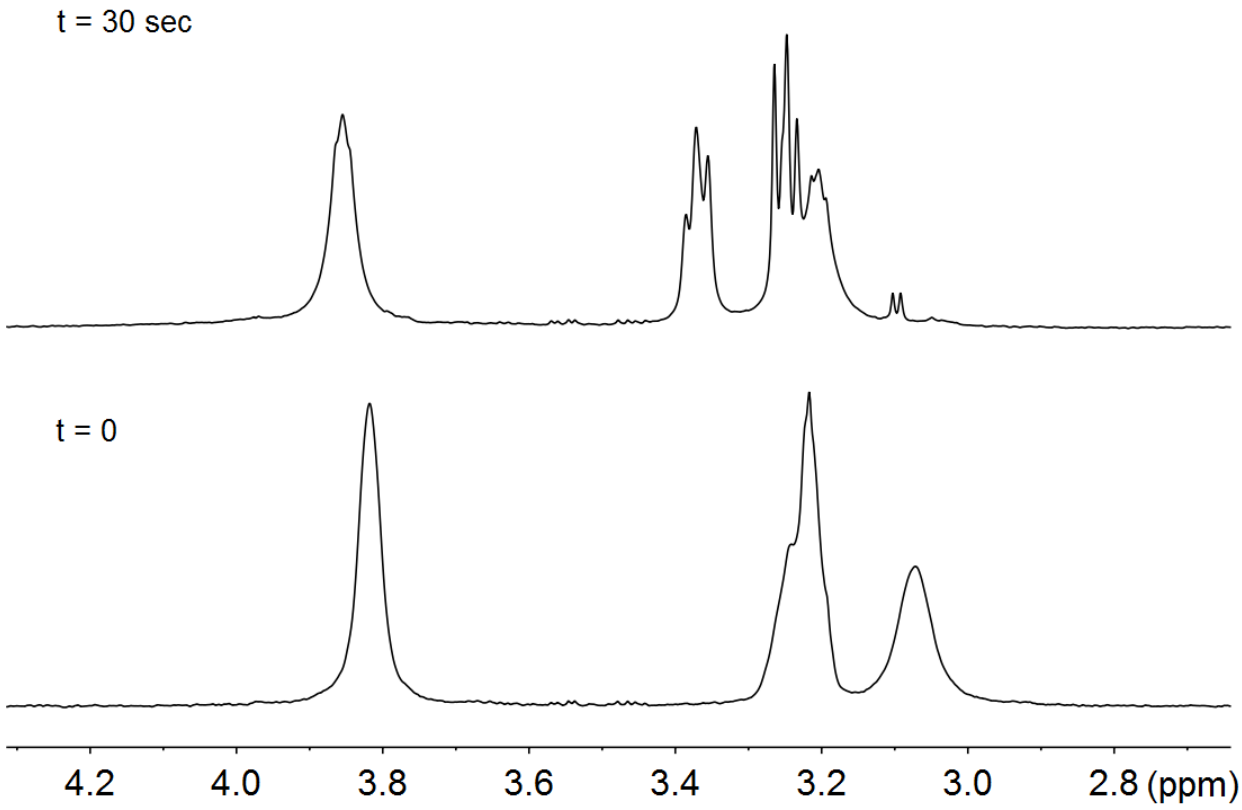

Figure S14. Light-induced MES oxidation by **Rf**. ^{1}H NMR spectra of a MES solution (3 mM) containing 500 µM **1** and 50 µM **Rf** under 460-nm light irradiation (2.5 mW·cm^{-2}) for t_{irr} = 0 and 30 sec. The newly formed peaks are assigned to oxidized MES species.

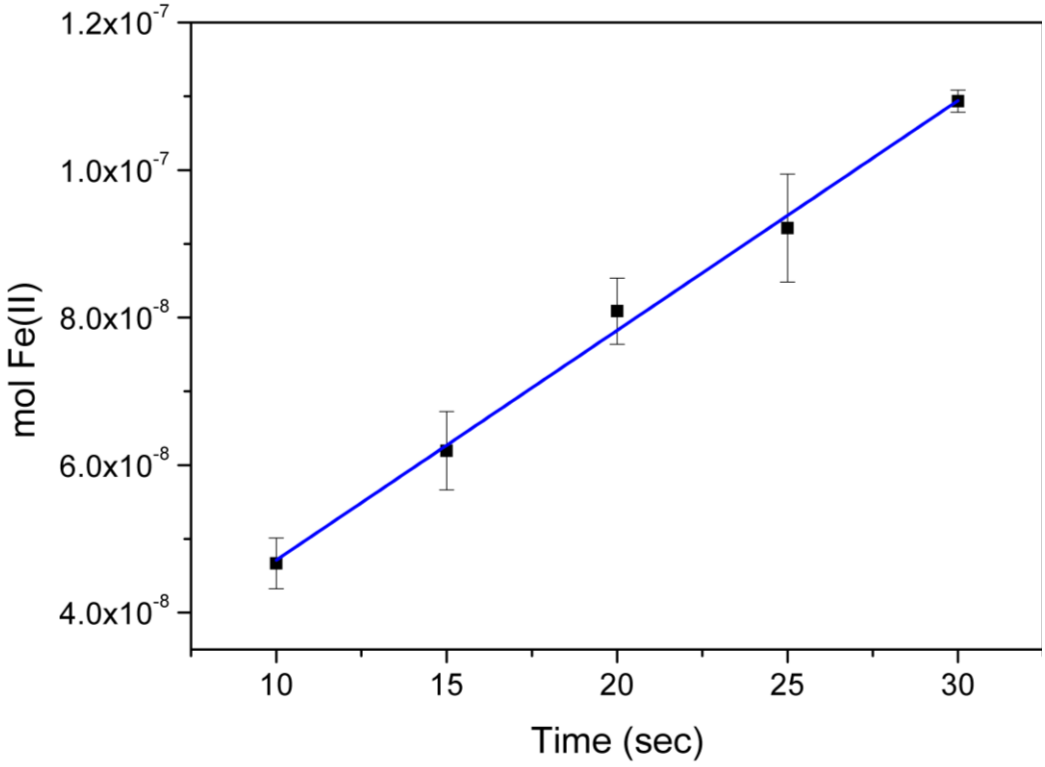

Figure S15. Plot of Fe(II) mol vs. irradiation time at 460 nm. The ferrioxalate actinometer ($K_3[Fe(C_2O_4)_3]$) (0.15 M) was irradiated with a 460-nm light source in a plate reader and a phenatroline-based developing solution was then added to determine spectrophotometrically the amount of Fe(II) ions generated by irradiation, as described by S. L. Hopkins et al.[3] Data were fitted with the equation y = $(3.12\cdot10^{-9} \pm 0.17\cdot10^{-9})$x + $(1.60\cdot10^{-8} \pm 4.52\cdot10^{-9})$. R-Square = 0.998. Being the absolute quantum yield $\Phi_{Fe(II)}$ for ($K_3[Fe(C_2O_4)_3]$) (0.15 M) at 460 nm equal to 0.65,[3] a photon flux of $8.09\cdot10^{-9} \pm 0.94\cdot10^{-9}$ mol photon·sec^{-1} was obtained for the light source using the equation:

$$\Phi_{Fe(II)} = \frac{\eta_{Fe(II)}}{I_{abs}}$$

where $\eta_{Fe(II)}$ the moles of Fe(II) produced photochemically and I_{abs} the absorbed photon dose by the Fe-oxalate complex.[4]

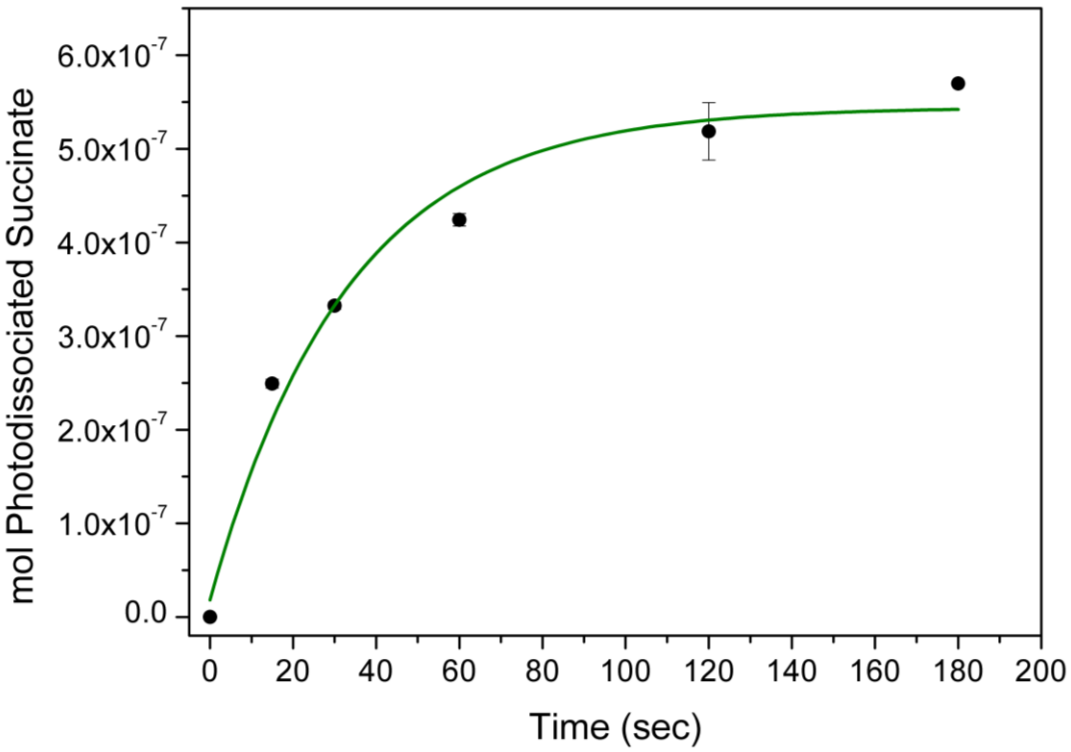

Figure S16. Moles of photodissociated succinate ligand vs. irradiation time at 460 nm. MES (18 mM) solutions of **1** (1.00 mM) and **Rf** (50 µM) placed in a plate reader were irradiated at 460 nm for different time intervals and using the same setup employed for the ferrioxalate actinometry. The amount of photodissociated succinate was quantified by ^{1}H NMR spectroscopy and data were fitted with the equation $y = (-5.26 \cdot 10^{-7} \pm 4.2 \cdot 10^{-8})e^{\frac{-x}{32.89 \pm 6.45}} + (-5.44 \cdot 10^{-7} \pm 2.9 \cdot 10^{-8})$. R-Square = 0.969.

By employing the equation

$$\phi = \frac{\text{number of molecules (or moles)consumed or produced per unit time}}{\text{number of photons adsorbed per unit time}} = \frac{\frac{d}{dt}\frac{[\text{Succinate}]}{2}}{\text{Lamp Intensity}}$$

a quantum yield ϕ of 1.4 ± 0.1 was determined.

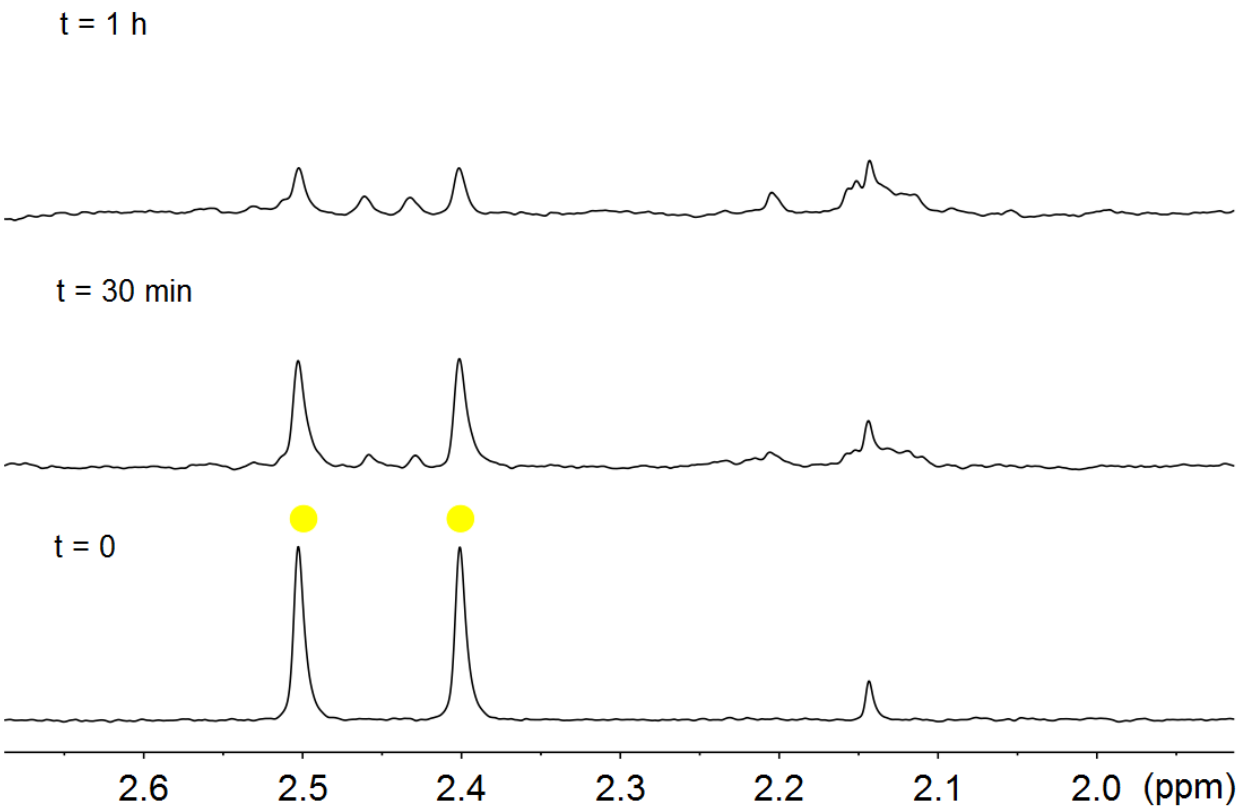

Figure S17. Photostability of **Rf** in MES buffer. ^{1}H NMR spectra of a MES/D_2O (9:1, MES 18 mM, pH 6.0) solution of 240 μM **Rf** under 460-nm light irradiation (2.5 mW·cm^{-2}) for t_{irr} = 0, 30 and 60 min. ^{1}H NMR signal labelling: ● methyl groups of **Rf** isoalloxazine ring.

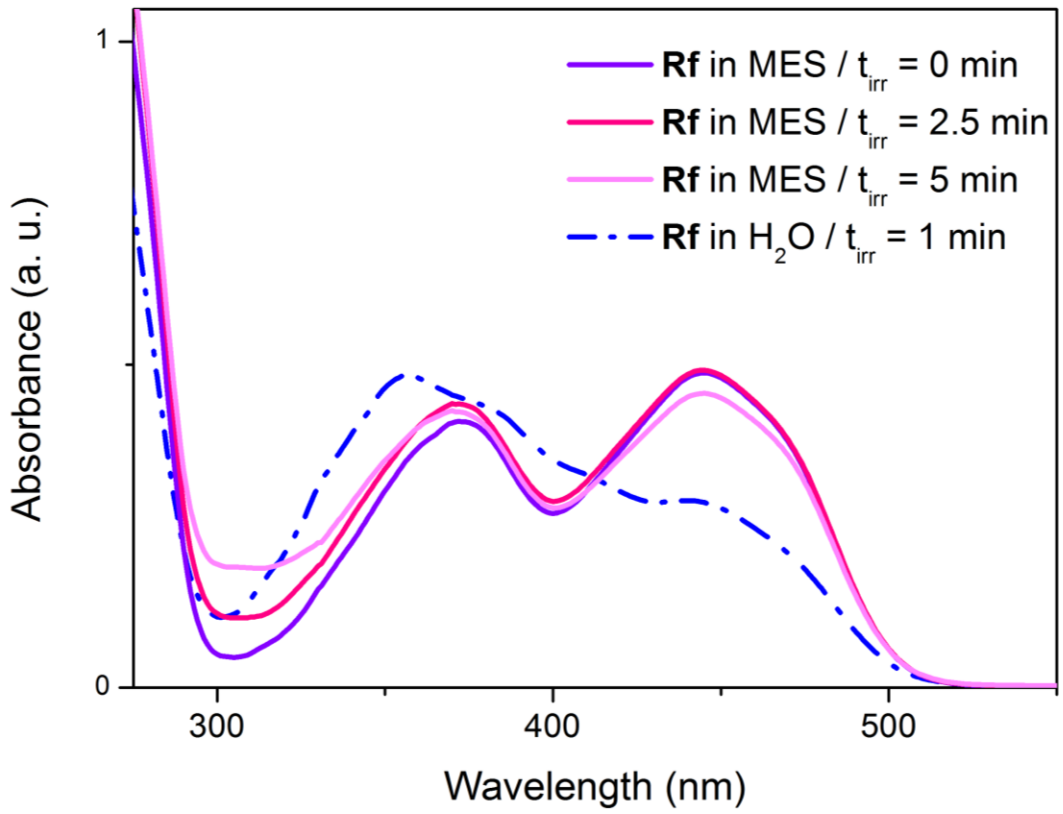

Figure S18. Photostability of **Rf** in MES buffer and water. UV-Vis spectrum of **Rf** (50 µM) in MES buffer (20 mM, pH 6) and in water (pH 7) at different irradiation times (λ_{irr} = 460 nm, 2.5 mW·cm^{-2}; MES: violet t_{irr} = 0, magenta t_{irr} = 2.5 min, and pink t_{irr} = 5 min; Water: dashed-blue t_{irr} = 1 min). The absorption profile obtained after light irradiation in water (dashed blue line) corresponds to lumichrome, a common photoproduct of **Rf** photolysis.

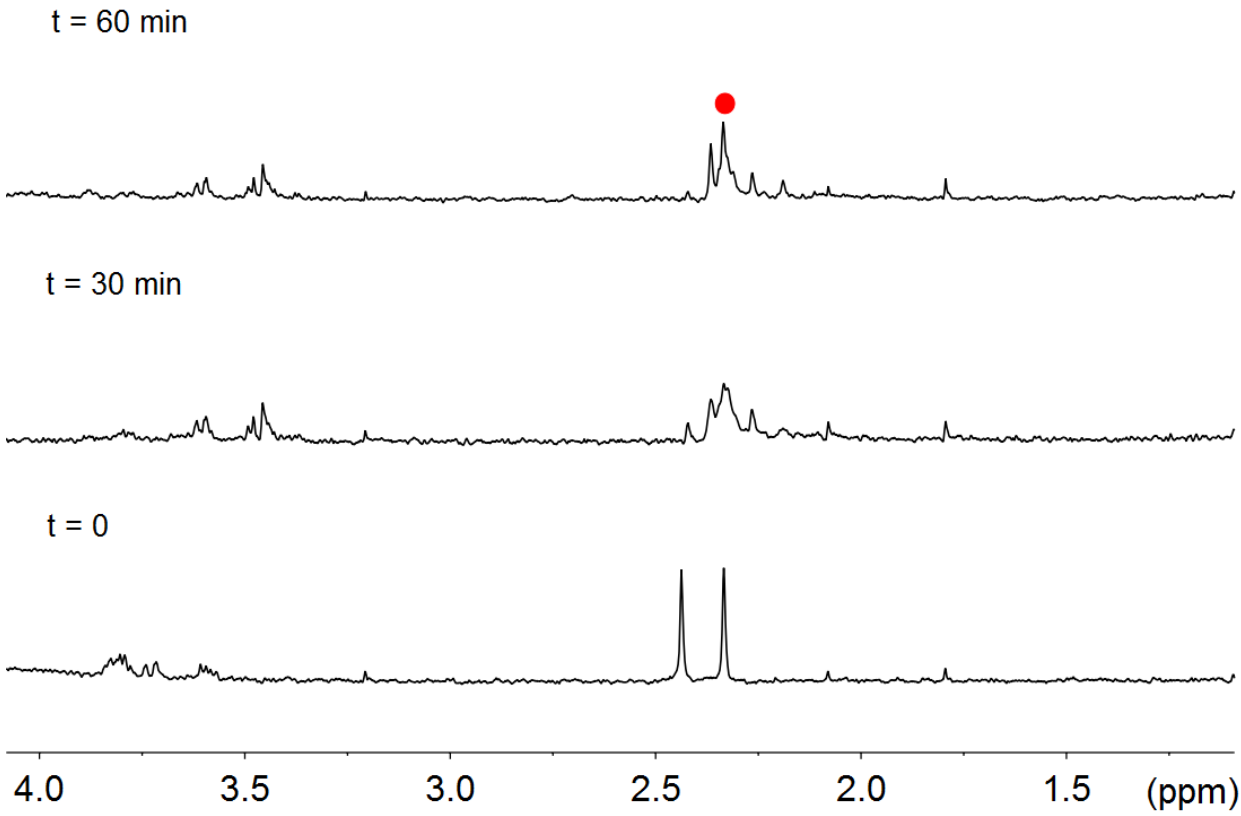

Figure S19. Photostability of **Rf** in Phosphate Buffer (PB). ^{1}H NMR spectra of a PB/D_2O (9:1, 100 mM, pH 5.5) solution of 240 µM **Rf** under 460-nm light irradiation (2.5 mW·cm^{-2}) for t_{irr} = 0, 30 and 60 min. Changes in the ^{1}H NMR signal at 3.5–3.8 ppm indicate the ribityl side chain is undergoing intramolecular photodegradation. Appearance of the peak at at 2.33 ppm (●) is consistent with the formation of 2,3-butanedione, a photoproduct obtained by O_2-oxidation of the isoalloxazine ring.

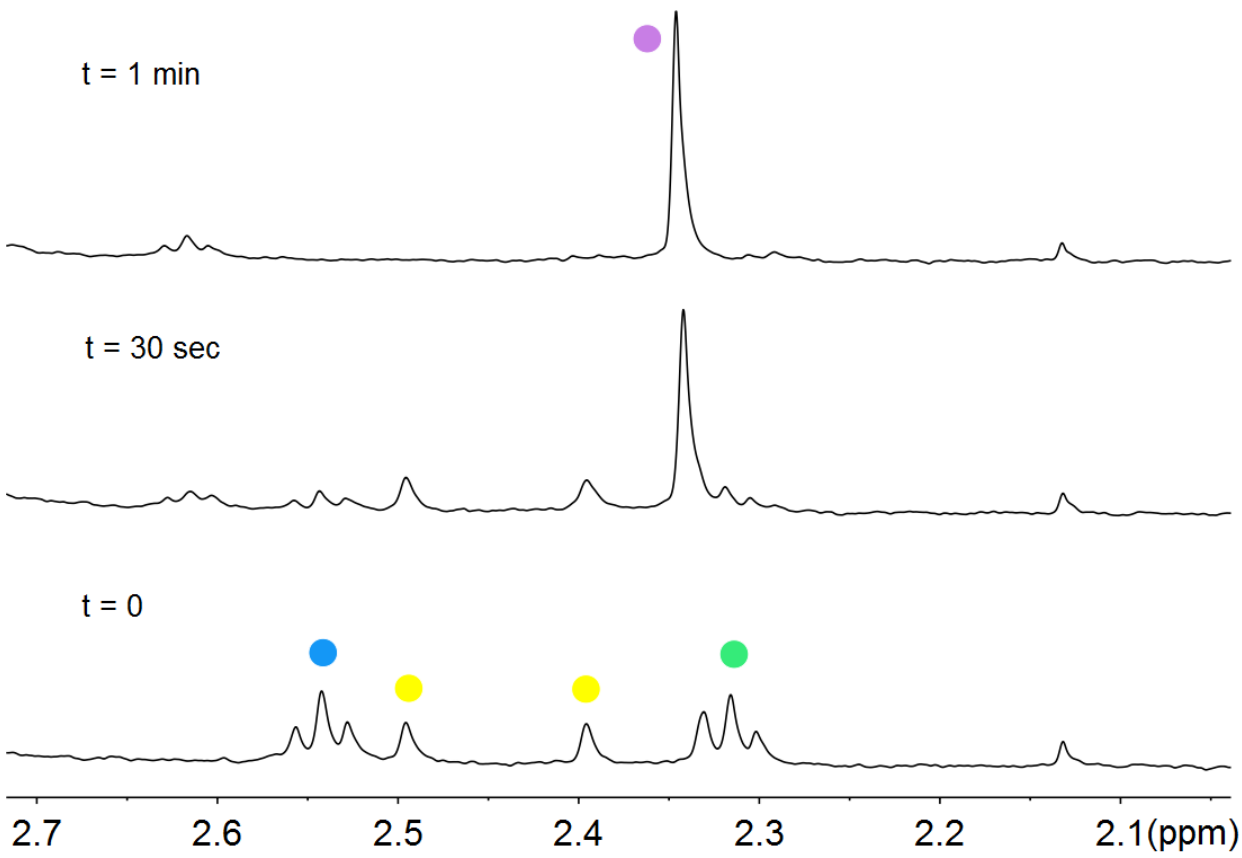

Figure S20. Photolysis of **1** in HEPES buffer in the presence of 50 μM **Rf**. ^{1}H NMR spectra of a HEPES/D_2O solution (9:1, HEPES 18 mM, pH 6.0) of 120 μM **1** and 50 μM **Rf** under 460-nm light irradiation (2.5 mW·cm^{-2}) for t_{irr} = 0 sec, 30 sec, 1 min. ^{1}H NMR signal labelling: ● Pt–OCO**CH$_2$**CH$_2$CO$_2^-$, ● Pt–OCOCH$_2$**CH$_2$**CO$_2^-$, ● methyl groups of **Rf** isoalloxazine ring, ● free $^-$O$_2$C**CH$_2$CH$_2$**CO$_2^-$.

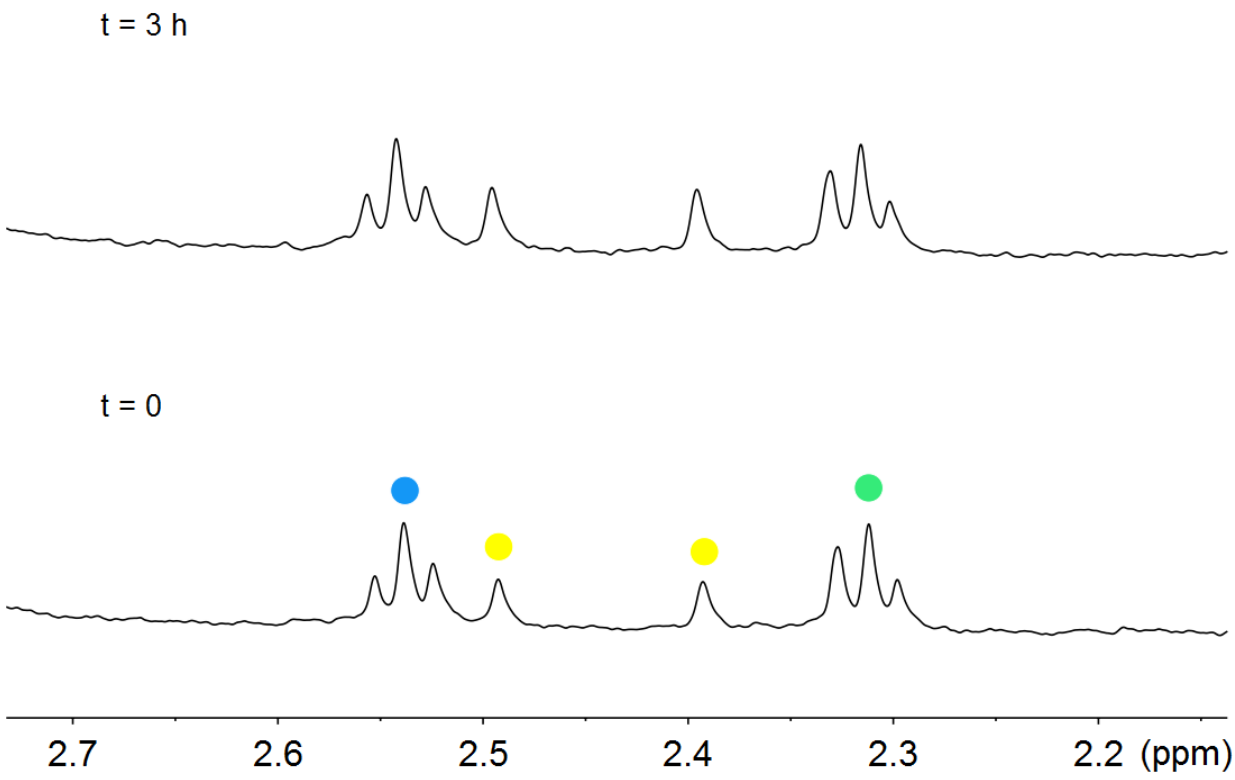

Figure S21. Stability control in the dark for **Rf/1** in HEPES buffer. ^{1}H NMR spectra of HEPES/D_2O solution (9:1, HEPES 18 mM, pH 6.0) containing 120 µM **1** and 50 µM **Rf** in the dark for t = 0 and 3 h. ^{1}H NMR signal labelling: ● Pt–OCO**C**$\mathbf{H_2}$$CH_2CO_2^-$, ● Pt–OCO$CH_2$**C**$\mathbf{H_2}$$CO_2^-$ and ● methyl groups of **Rf** isoalloxazine ring.

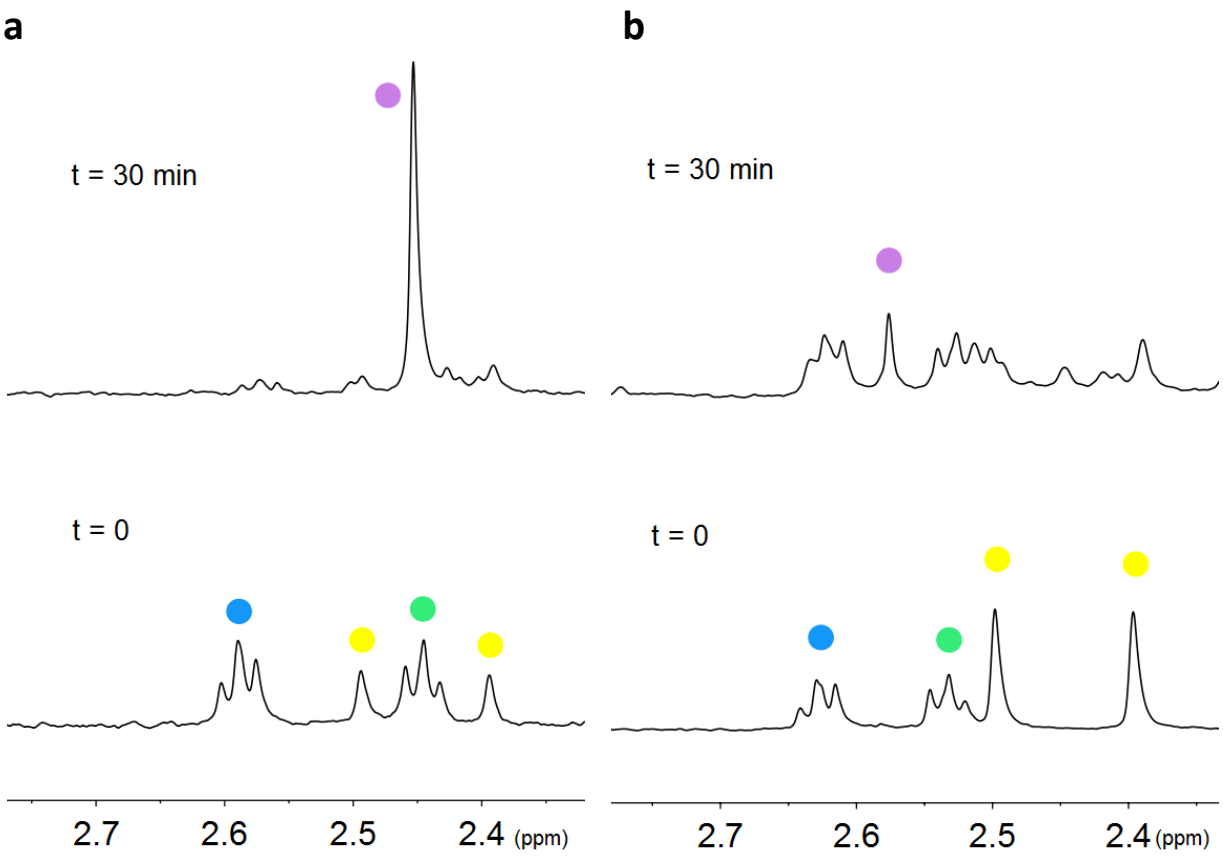

Figure S22. Photolysis of **1** in the presence of **Rf** and NaN_3 in water. (**a**) ^{1}H NMR spectra of a H_2O/D_2O (9:1, pH 3) solution of **Rf**/**1** (50/120 μM) with 3 mM NaN_3 under 460-nm light irradiation (2.5 mW·cm^{-2}) for t_{irr} = 0 and 30 min; (**b**) ^{1}H NMR spectra of a H_2O/D_2O (9:1, pH 2.7) solution of **Rf**/**1** (240/120 μM) without NaN_3 irradiated under the same conditions. In all experiments, HCOOH was added (3 mM and 24 mM for **a** and **b** respectively) to improve the photoconversion of **1** and slightly reduce the photodecomposition of **Rf**. ^{1}H NMR signal labelling: ● Pt–OCO**C**$\mathbf{H_2}$$CH_2CO_2^-$, ● Pt–OCO$CH_2$**C**$\mathbf{H_2}$$CO_2^-$, ● methyl groups of **Rf** isoalloxazine ring, ● free ^-O_2C**C**$\mathbf{H_2}$**C**$\mathbf{H_2}$$CO_2^-$.

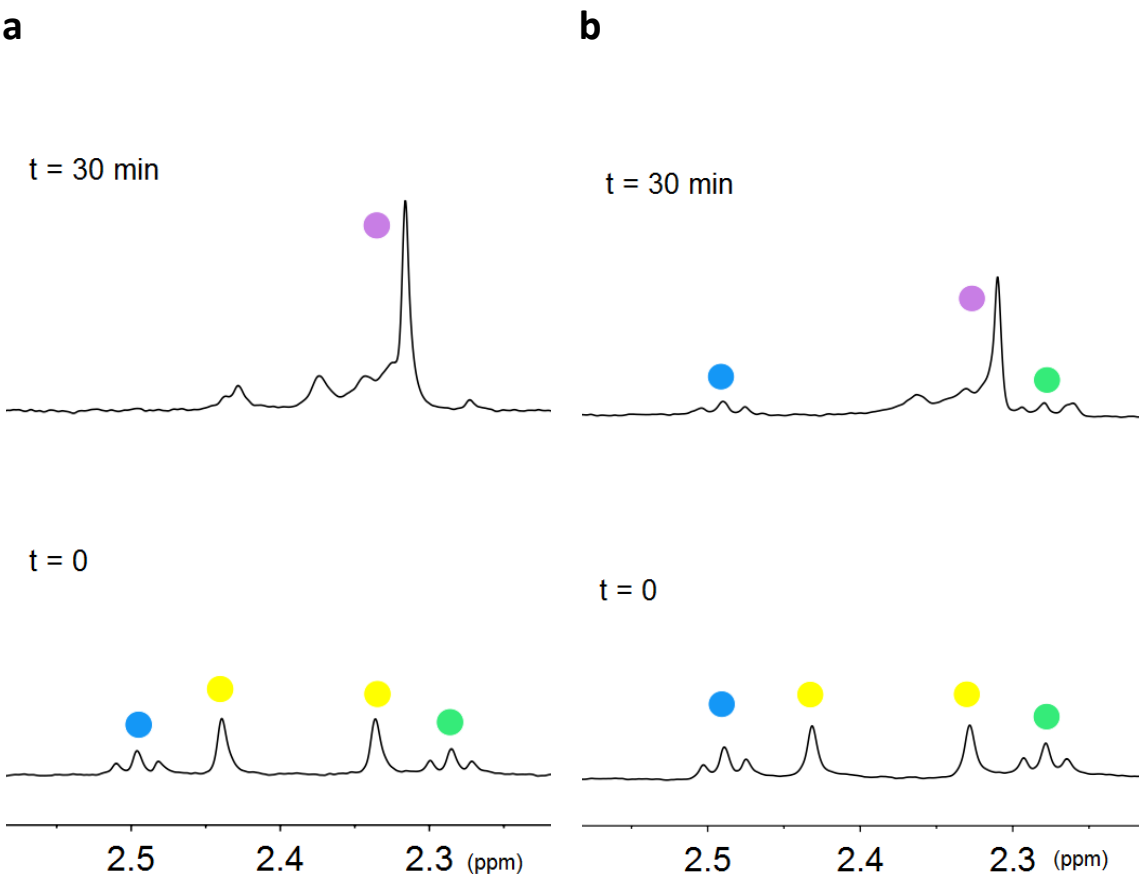

Figure S23. Photolysis of **1** in the presence of **Rf** and NaN_3 in Phosphate Buffer (PB). ^1H NMR spectra of a PB/D_2O (9:1, 100 mM, pH 5.5) solution of **Rf**/**1** (240/120 µM), with (**a**) or without (**b**) 1 mM NaN_3 under 460-nm light irradiation (2.5 mW·cm^{-2}) for t_{irr} = 0 and 30 min. In all experiments, 24 mM HCOOH was added to improve the photoconversion of **1** and slightly reduce the photodecomposition of **Rf**. ^1H NMR signal labelling: ● Pt–OCO**CH$_2$**CH$_2$CO$_2^-$, ● Pt–OCOCH$_2$**CH$_2$**CO$_2^-$, ● methyl groups of **Rf** isoalloxazine ring, ● free $^-$O$_2$C**CH$_2$CH$_2$**CO$_2^-$.

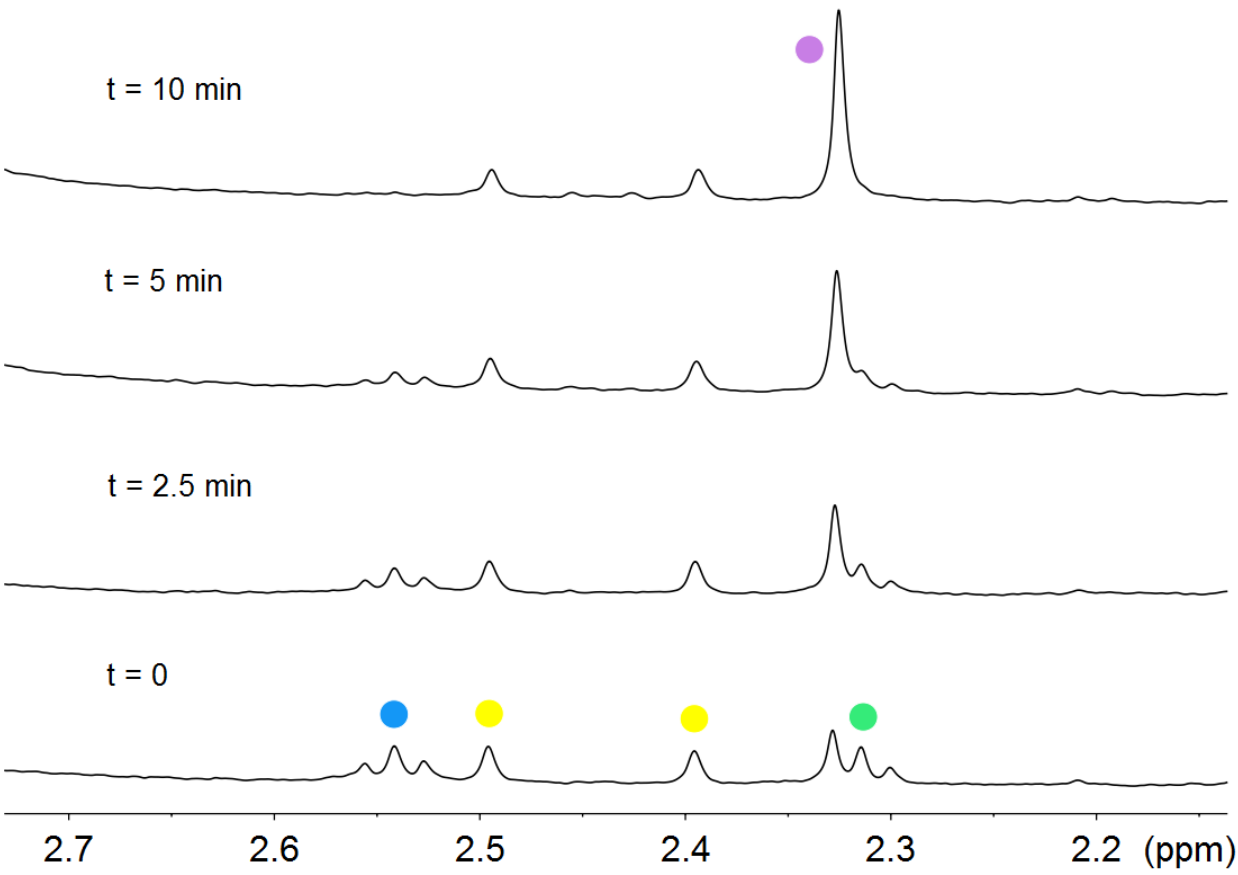

Figure S24. Photolysis of **1** in MES buffer in the presence of **Rf** and NaN_3. ^1H NMR spectra of a MES/D_2O (9:1, 18 mM, pH 6.0) solution of **Rf**/**1** (50/120 µM) with 18 mM NaN_3 under 460-nm light irradiation (2.5 $mW \cdot cm^{-2}$) for t_{irr} = 0, 2.5, 5 and 10 min. ^1H NMR signal labelling: ● Pt–$OCO\mathbf{CH_2}CH_2CO_2^-$, ● Pt–$OCOCH_2\mathbf{CH_2}CO_2^-$, ● methyl groups of **Rf** isoalloxazine ring, ● free $^-O_2C\mathbf{CH_2CH_2}CO_2^-$.

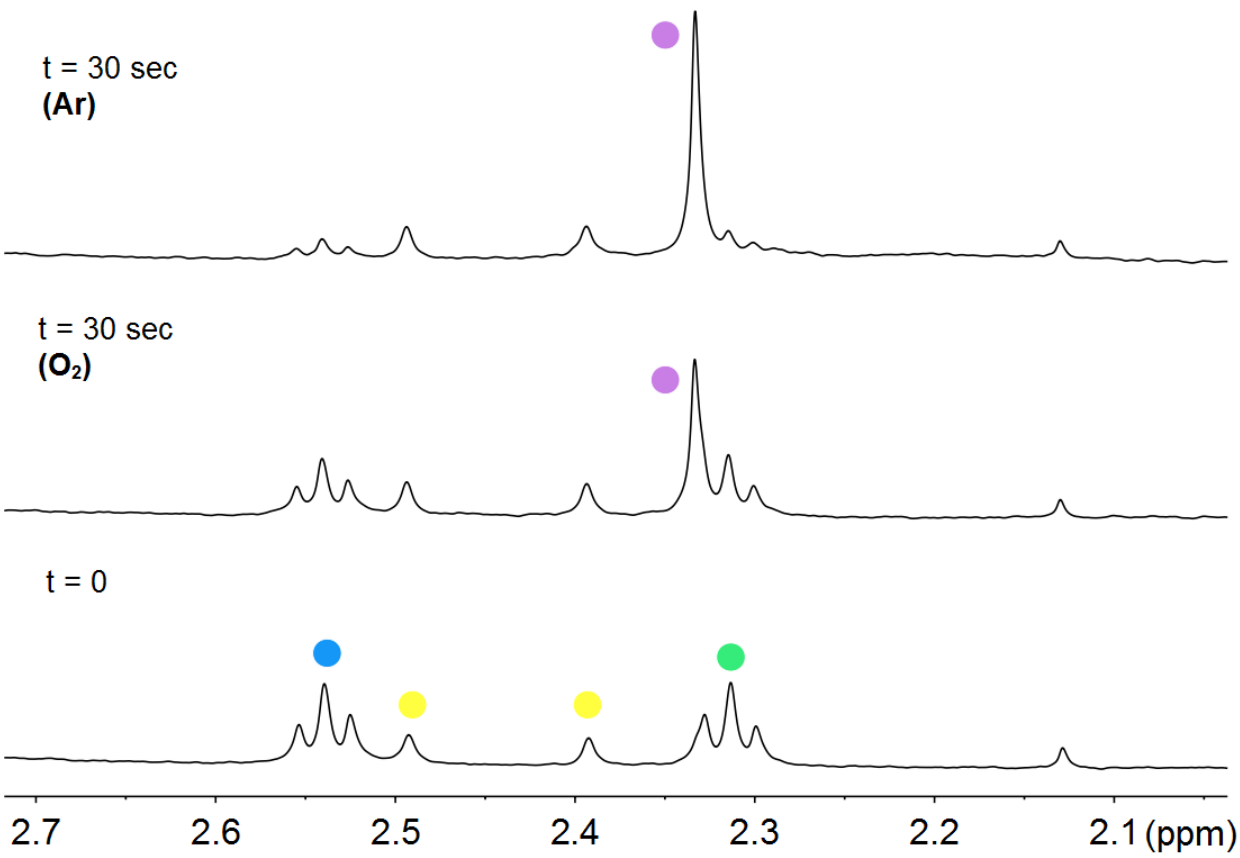

Figure S25. Photolysis of **1** in MES buffer in the presence of **Rf** under Ar atmosphere or in air. ^{1}H NMR spectra of a MES/D_2O (9:1, 18 mM, pH 6.0) solution of **Rf**/**1** (50/200 μM) under 460-nm light irradiation (6 mW·cm^{-2}) for t_{irr} = 0 and 30 sec. ^{1}H NMR signal labelling: ● Pt–OCO**CH_2**CH_2CO_2^-, ● Pt–OCOCH_2**CH_2**CO_2^-, ● methyl groups of **Rf** isoalloxazine ring, ● free $^-$O$_2$C**CH_2CH_2**CO_2^-.

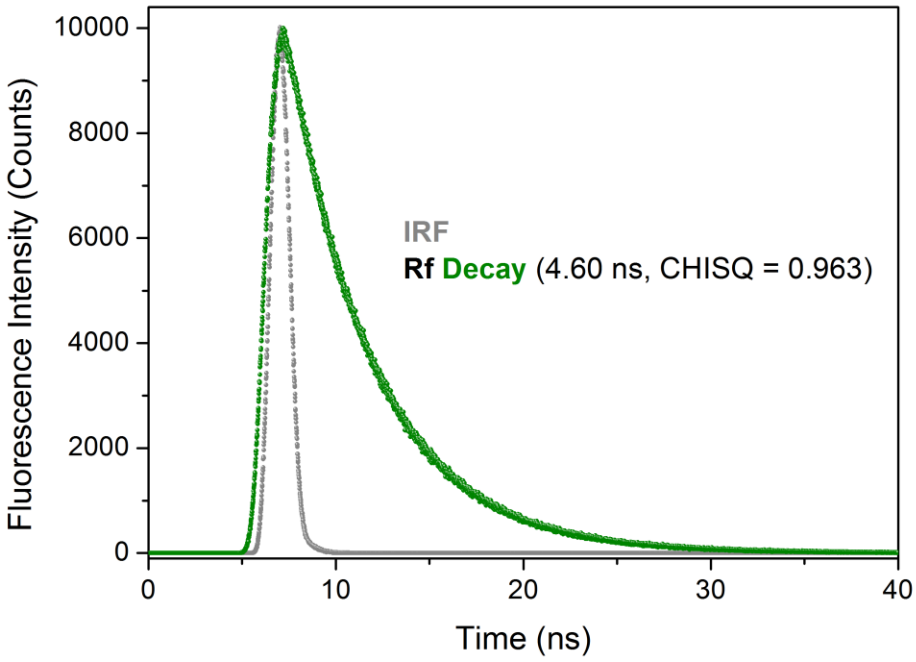

Figure S26. Lifetime decay profile for **Rf**. Fluorescence lifetime measurement for a 5 μM **Rf** solution in MES buffer (10 mM) measured in a time-correlated single photon counting (TCSPC) setup. **Rf** exhibits a mono-exponential decay with a lifetime of 4.60 nm (green dots). IRF (grey dots) = instrument response function (prompt).

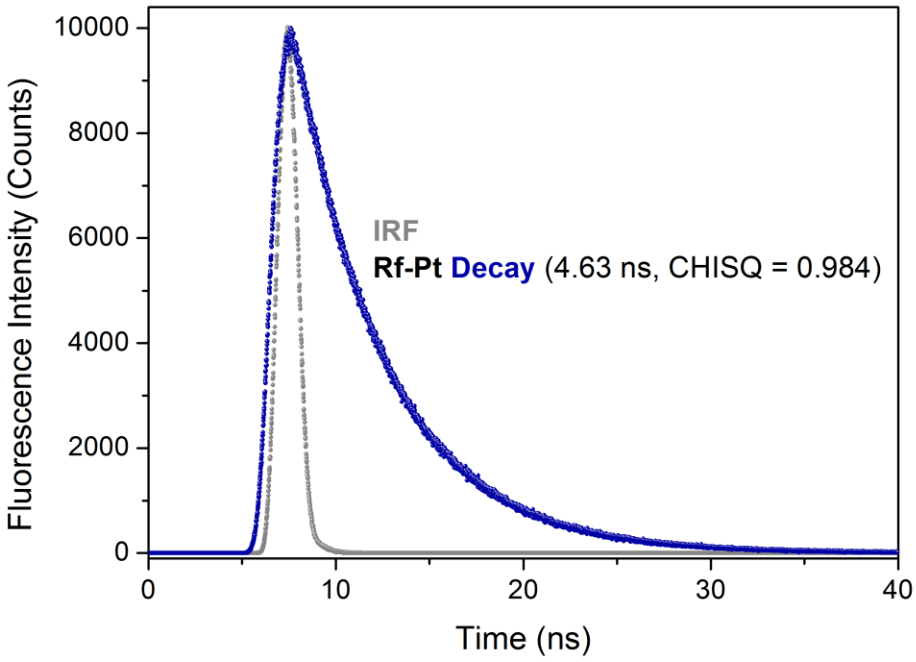

Figure S27. Lifetime decay profile for **Rf** in the presence of **1**. Fluorescence lifetime measurement for a 5 μM **Rf** solution in MES buffer (10 mM) measured in the presence of 1.8 mM of **1** in a time-correlated single photon counting (TCSPC) setup. **Rf** exhibits a mono-exponential decay with a lifetime of 4.63 nm (blue dots). IRF (grey dots) = instrument response function (prompt).

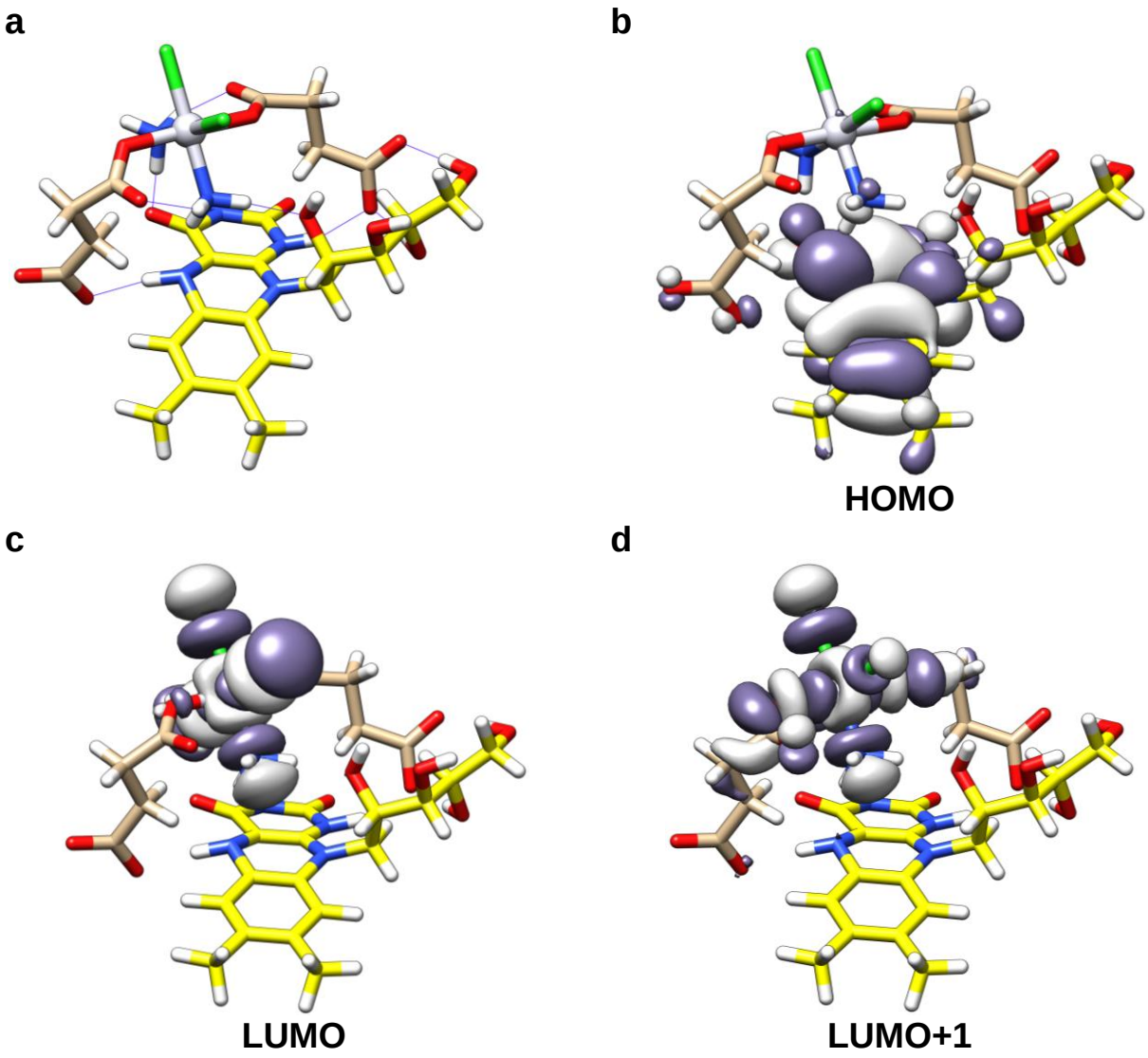

Figure S28. DFT-optimized structure and frontier orbitals of a selected **1-RfH$_2$** adduct. (**a**) Conformation of a selected **1-Rf**H$_2$ adduct optimized by DFT at the PBE0/def2-SVP[1,2] level (H-bond contacts highlighted with violet lines). (**b–d)** Frontier orbitals for the optimized conformation of the **1-Rf**H$_2$ adduct (isodensity surfaces plotted with the isovalue of 0.02 $e^{-}\cdot bohr^{-3}$). The stabilization energy for **1-Rf**H$_2$ is –52.0 $kcal\cdot mol^{-1}$ and is calculated using the formula $\Delta E = E_{\mathbf{1\text{-}RfH2}} - (E_{\mathbf{1}} + E_{\mathbf{RfH2}})$.

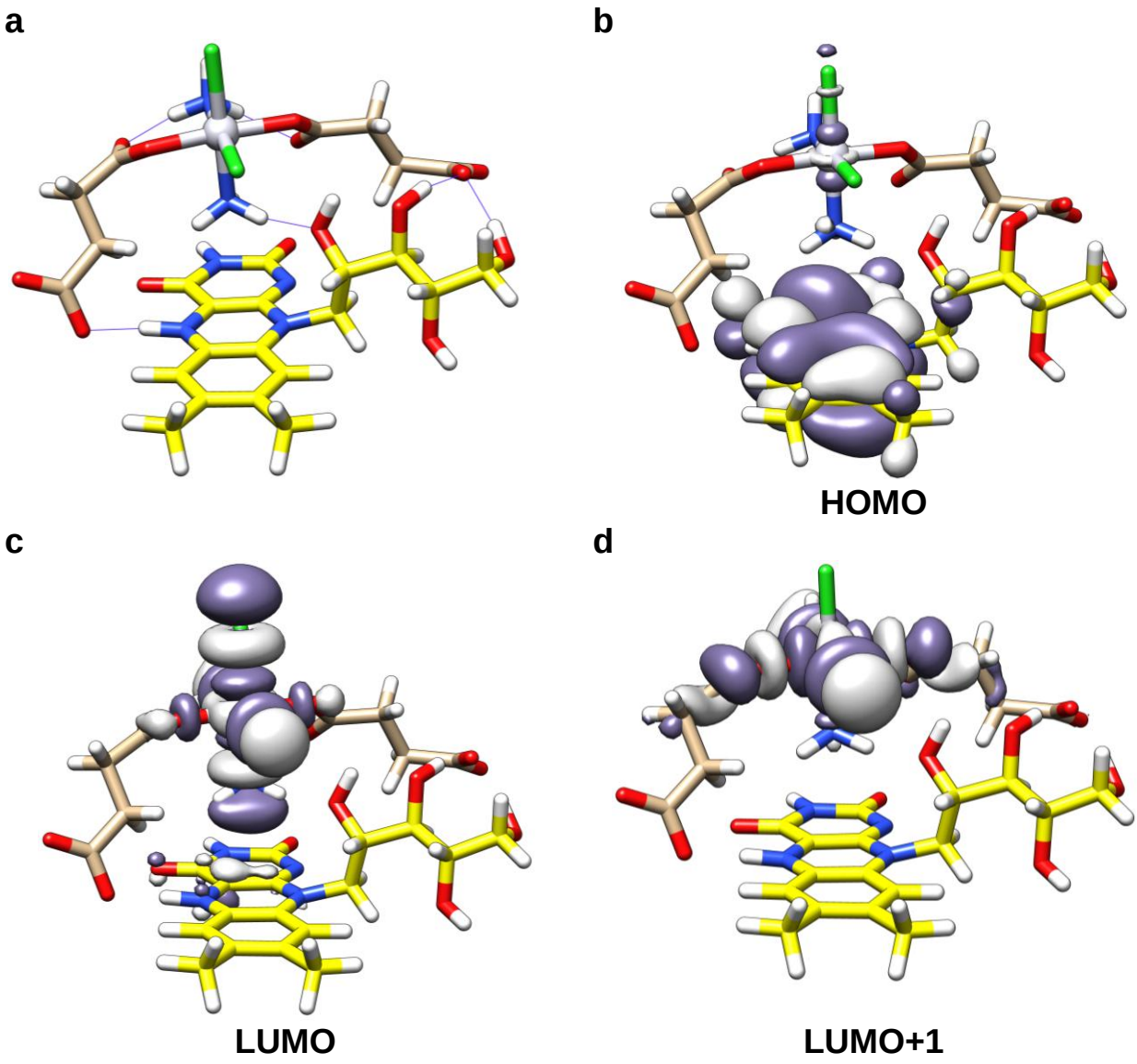

Figure S29. DFT-optimized structure and frontier orbitals of a selected **RfH**$^{-}$ adduct (N5). **(a)** Conformation of a selected **1-RfH**$^{-}$ adduct (N5-protonated) optimized by DFT at the PBE0/def2-SVP[1,2] level (H-bond contacts highlighted with violet lines). (**b–d)** Frontier orbitals for the optimized conformation of the **1-RfH**$^{-}$ adduct (isodensity surfaces plotted with the isovalue of 0.02 $e^{-}\cdot bohr^{-3}$). The stabilization energy for **1-RfH**$^{-}$ is –68.8 $kcal\cdot mol^{-1}$ and is calculated using the formula $\Delta E = E_{\mathbf{1\text{-}RfH}} - (E_{\mathbf{1}} + E_{\mathbf{RfH}})$.

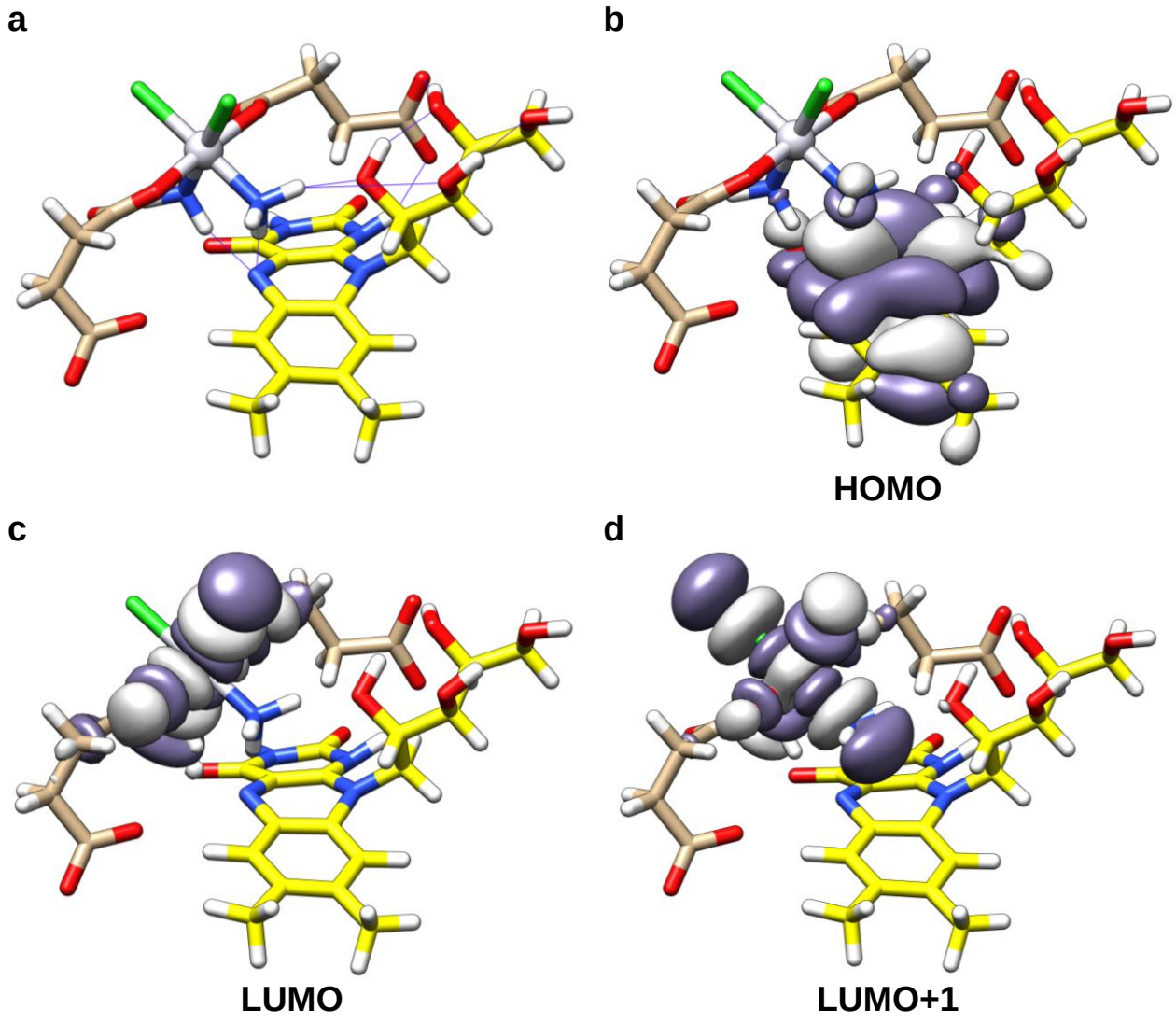

Figure S30. DFT-optimized structure and frontier orbitals of a selected **RfH**$^{-}$ adduct (N1). (**a)** Conformation of a selected **1**-**RfH**$^{-}$ adduct (N1-protonated) optimized by DFT at the PBE0/def2-SVP[1,2] level (H-bond contacts highlighted with violet lines). (**b–d)** Frontier orbitals for the optimized conformation of the **1**-**RfH**$^{-}$ adduct (isodensity surfaces plotted with the isovalue of 0.02 $e^{-}\cdot bohr^{-3}$). The stabilization energy for **1**-**RfH**$^{-}$ is –61.2 $kcal\cdot mol^{-1}$ and is calculated using the formula $\Delta E = E_{\mathbf{1\text{-}RfH}} - (E_{\mathbf{1}} + E_{\mathbf{RfH}})$.

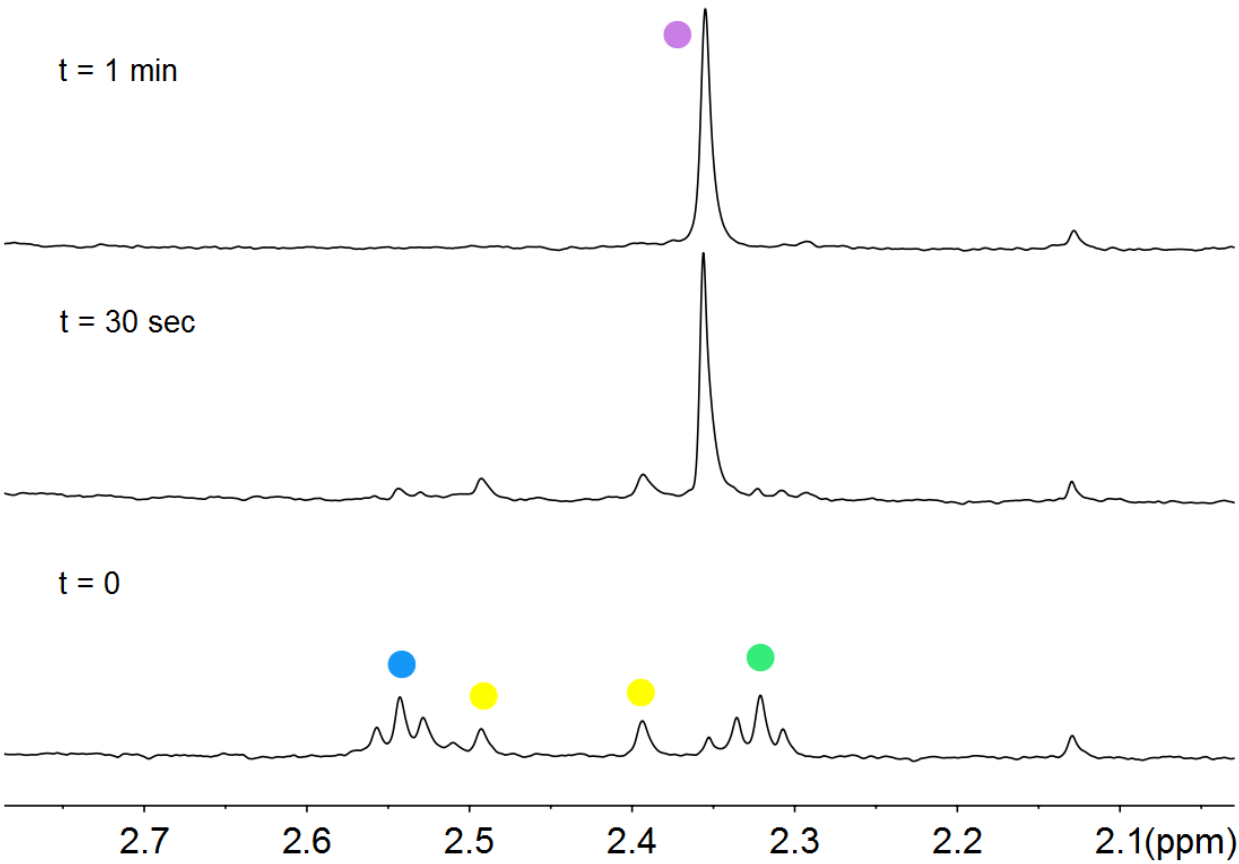

Figure S31. Photolysis of **1** in MES buffer in the presence of 50 μM FMN. ^{1}H NMR spectra of a MES/D_2O solution (9:1, MES 18 mM, pH 6.0) of 120 μM **1** and 50 μM FMN under 460-nm light irradiation (2.5 mW·cm^{-2}) for t_{irr} = 0 sec, 30 sec and 1 min. ^{1}H NMR signal labelling: ● Pt–OCO**CH$_2$**CH$_2$CO$_2^-$, ● Pt–OCOCH$_2$**CH$_2$**CO$_2^-$, ● methyl groups of FMN isoalloxazine ring and ● free $^-$O$_2$C**CH$_2$CH$_2$**CO$_2^-$.

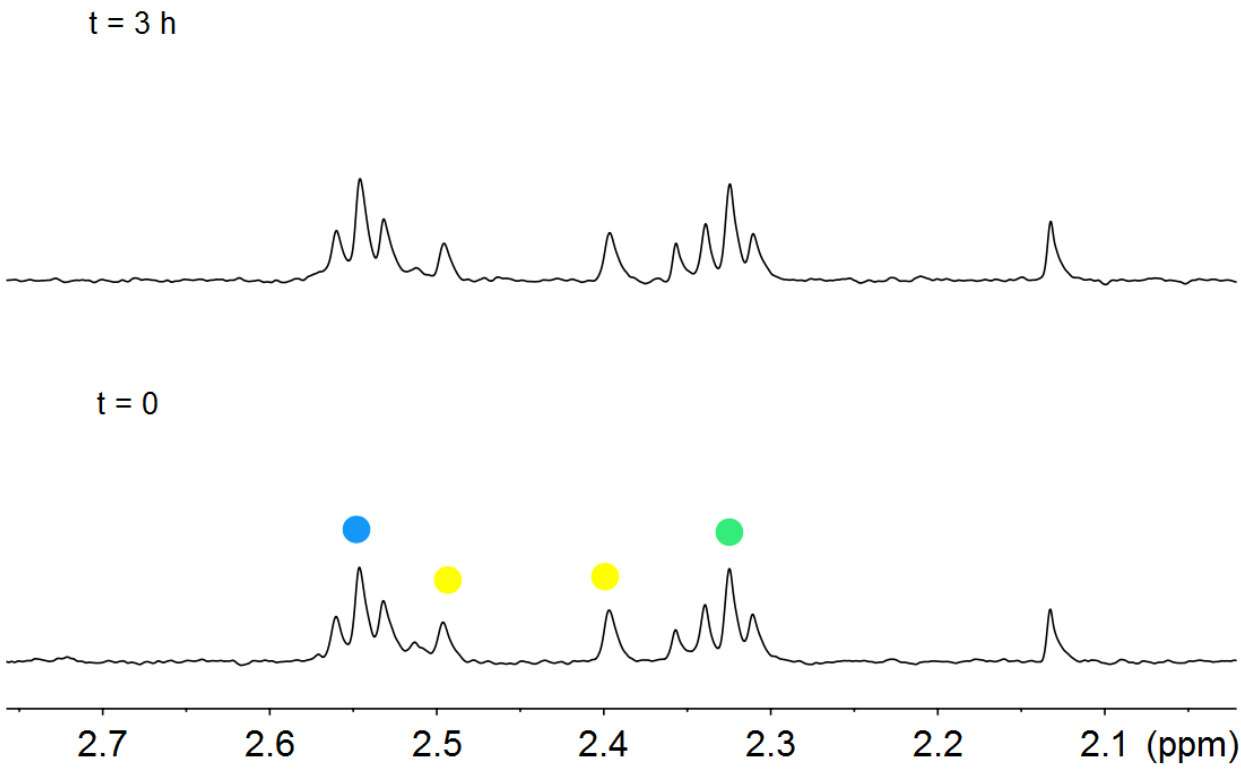

Figure S32. Stability of **1** in MES buffer in the presence of 50 µM FMN. ^{1}H NMR control spectra of a MES/D_2O solution (9:1, MES 18 mM, pH 6.0) of 120 µM **1** and 50 µM FMN in the dark for 3 h. ^{1}H NMR signal labelling: ● Pt–OCO**CH$_2$**$CH_2CO_2^-$, ● Pt–$OCOCH_2$**CH$_2$**CO_2^-, ● methyl groups of FMN isoalloxazine ring.

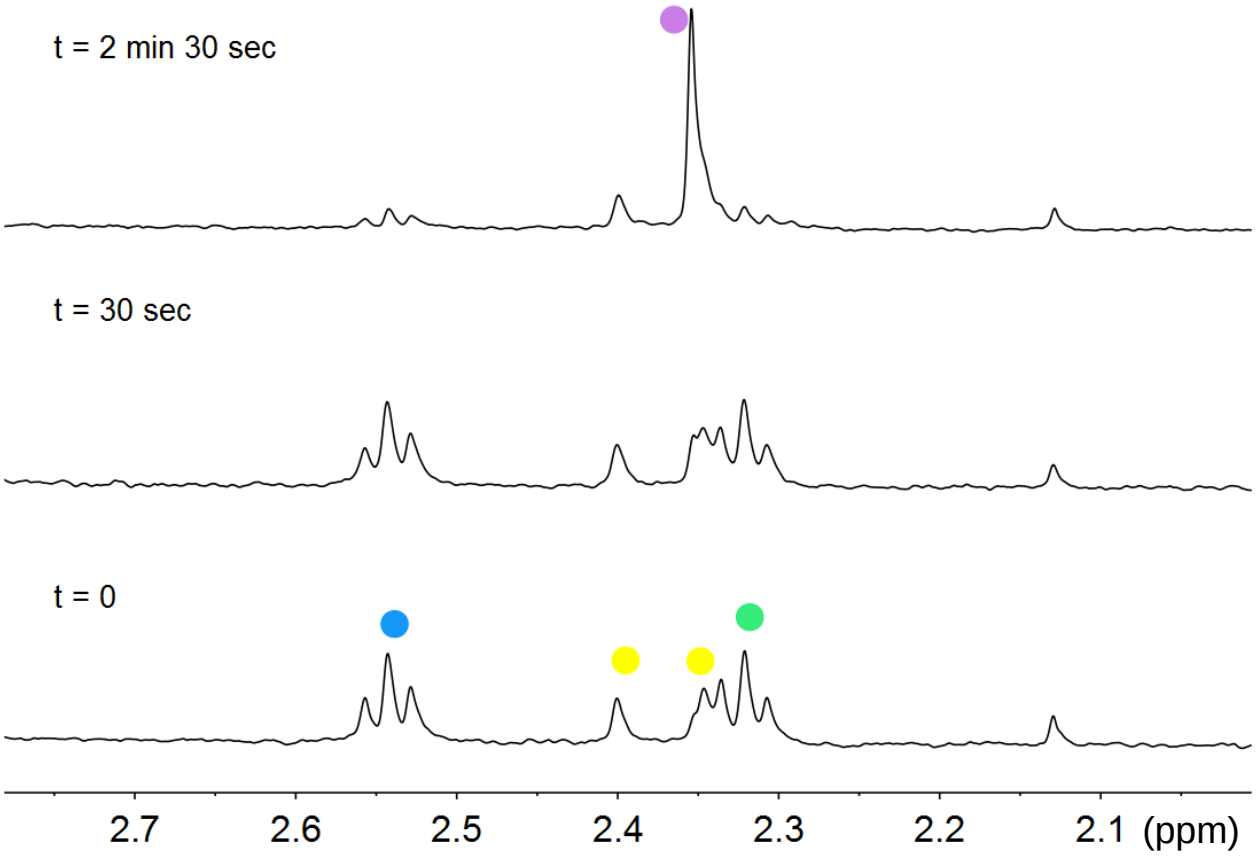

Figure S33. Photolysis of **1** in MES buffer in the presence of 50 μM FAD. ^{1}H NMR spectra of a MES/D_2O solution (9:1, MES 18 mM, pH 6.0) of 120 μM **1** and 50 μM FAD under 460-nm light irradiation (2.5 mW·cm^{-2}) for t_{irr} = 0 sec, 30 sec and 2.5 min. ^{1}H NMR signal labelling: ● Pt–OCO**CH$_2$**CH$_2$CO$_2^-$, ● Pt–OCOCH$_2$**CH$_2$**CO$_2^-$, ● methyl groups of FAD isoalloxazine ring and ● free $^-$O$_2$C**CH$_2$CH$_2$**CO$_2^-$.

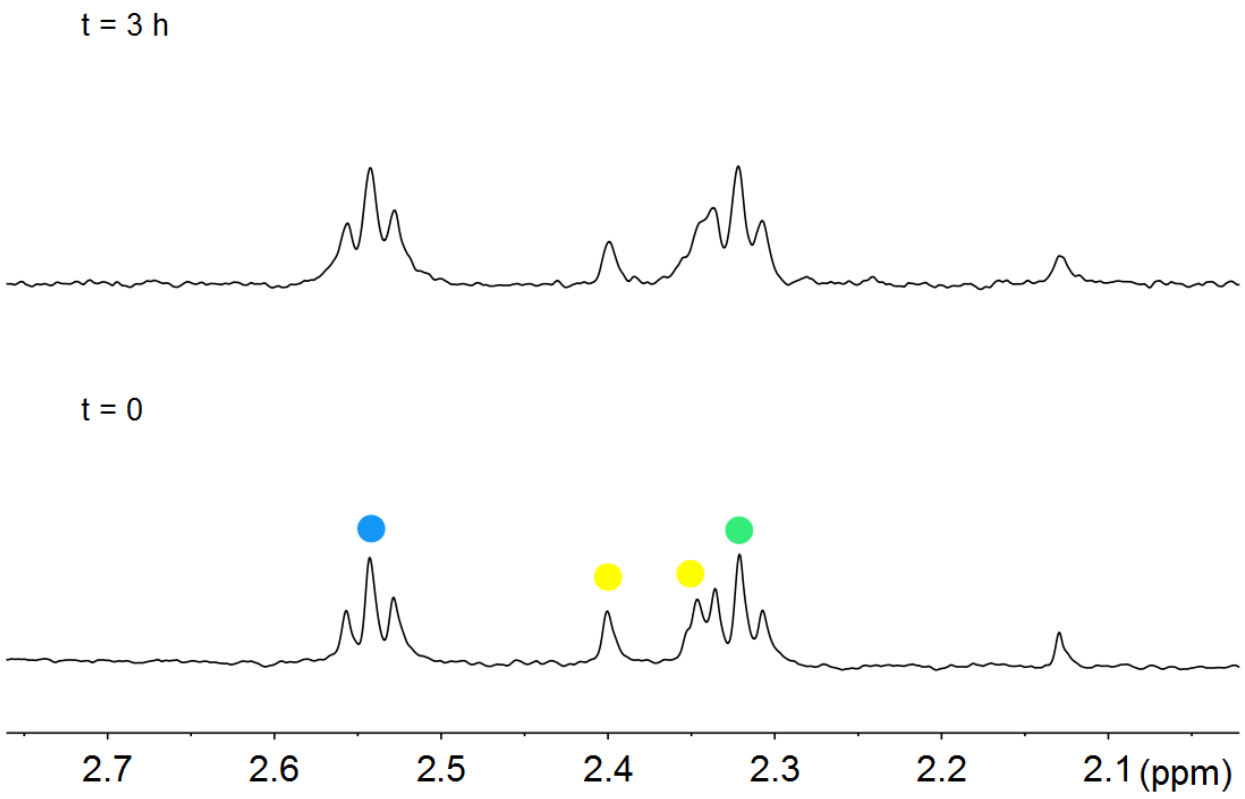

Figure S34. Stability of **1** in MES buffer in the presence of 50 µM FAD. ^{1}H NMR control spectra of a MES/D_2O solution (9:1, MES 18 mM, pH 6.0) of 120 µM **1** and 50 µM FAD in the dark for 3 h. ^{1}H NMR signal labelling: ● Pt–OCO**CH$_2$**$CH_2CO_2^-$, ● Pt–$OCOCH_2$**CH$_2$**CO_2^-, ● methyl groups of FAD isoalloxazine ring.

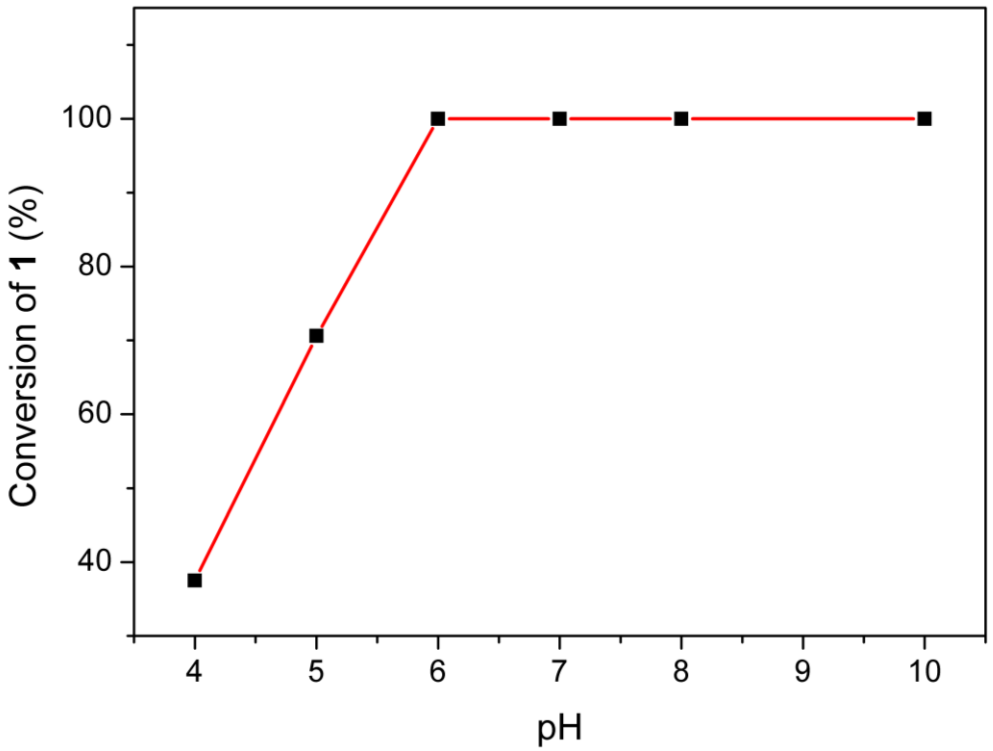

Figure S35. Dependency of photocatalytic prodrug activation on pH. Photocatalytic activation of **1** at different pHs (4-10) and at a fixed concentration of **Rf** (50 μM), **1** (120 μM) and MES (18 mM). An irradiation time of 2 min and 30 sec was set for all the samples (λ_{exc} = 460 nm, 2.5 mW·cm^{-2}).

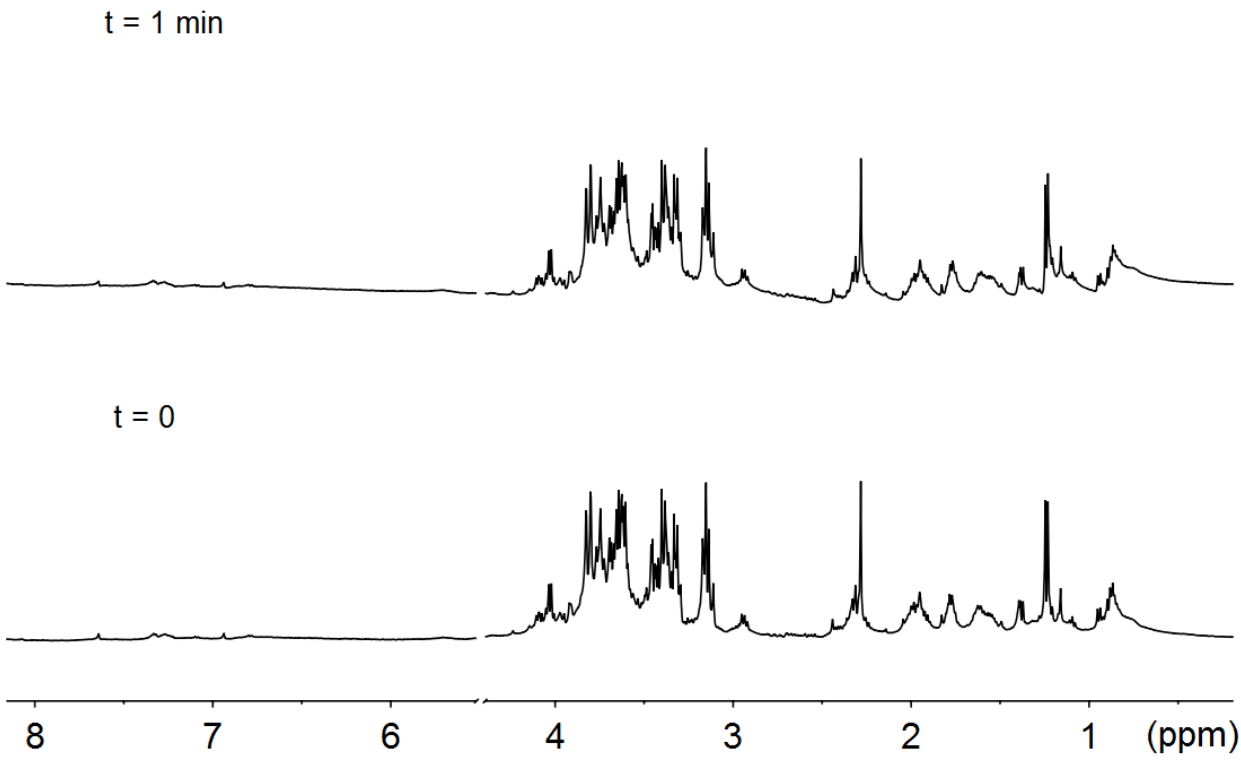

Figure S36. Photostability of cell culture medium. ^{1}H NMR spectra of cell culture medium (Ham's F-12K supplemented with 10% fetal bovine serum and 1% penicillin/streptomycin) before and after 1 min of irradiation with 460-nm light (6 mW·cm^{-2}).

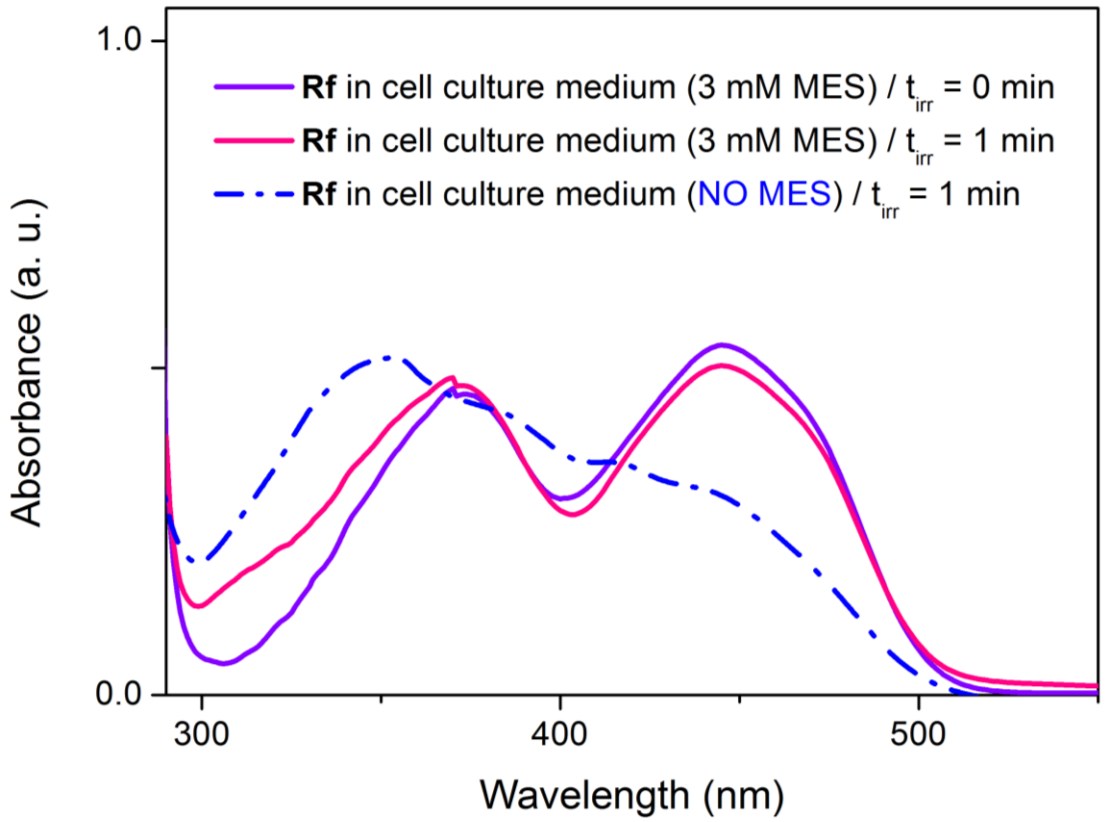

Figure S37. Photostability of **Rf** in cell culture medium. UV-Vis spectra of **Rf** (50 μM) in cell culture medium (Ham's F-12K supplemented with 10% fetal bovine serum and 1% penicillin/streptomycin) with 3 mM MES in the dark (violet line), after 1 min of irradiation (pink line) at 460 nm (6 mW·cm^{-2}) and after 1 min of irradiation in the absence of MES (blue line) at 460 nm (6 mW·cm^{-2}).

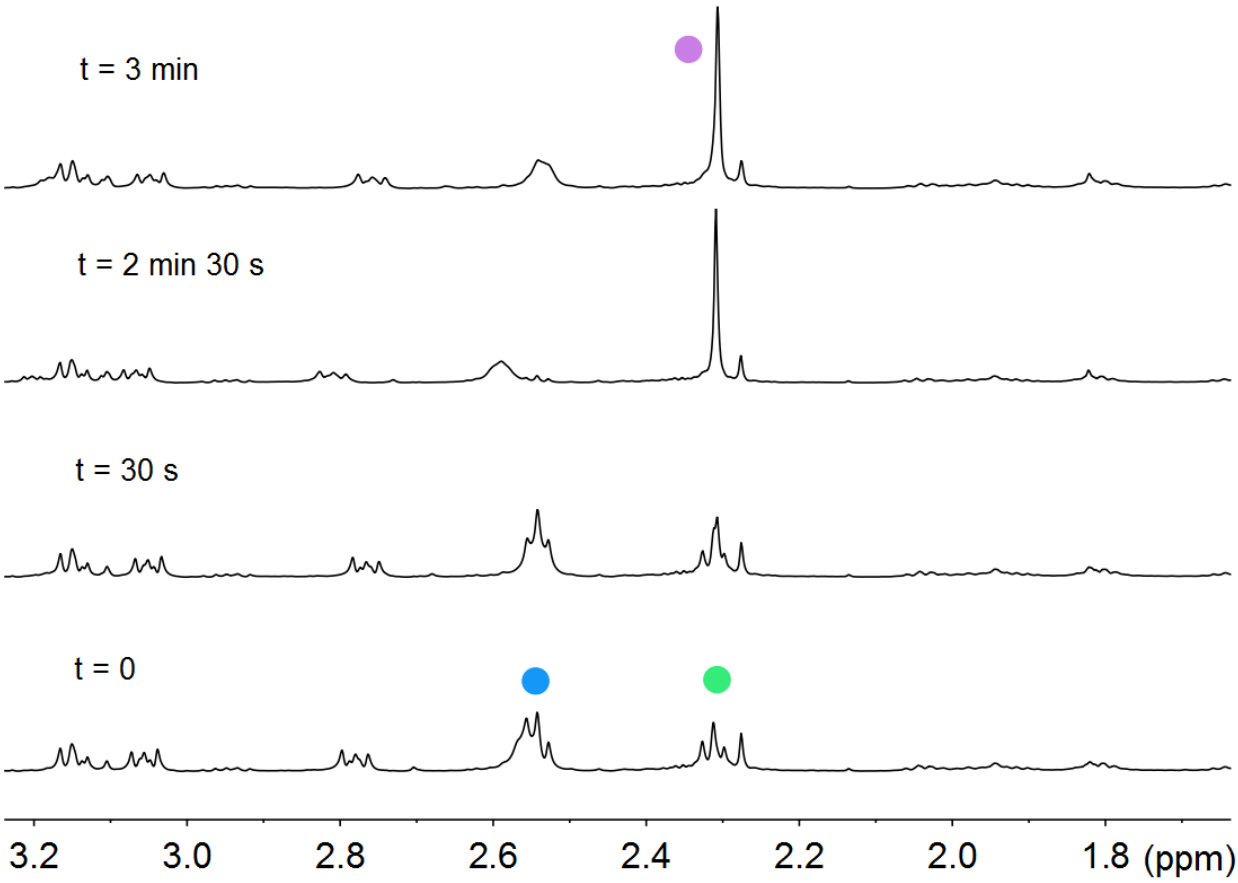

Figure S38. Photolysis of **1** in cell culture medium in the presence of **Rf** and MES. ^{1}H NMR spectra of cell culture medium/MES/D_2O (7.5:1.5:1, 3 mM MES) solution containing 1.92 mM **1** and 50 μM **Rf** under 460-nm light irradiation (6 mW·cm^{-2}) for t_{irr} = 0, 30 sec, 2.5 min and 3 min. Cell culture medium corresponds to Ham's F-12K medium supplemented with 10% fetal bovine serum and 1% penicillin/streptomycin. ^{1}H NMR signal labelling: ● Pt–OCO**C**$\mathbf{H_2}$$CH_2CO_2^-$, ● Pt–OCOC$H_2$**C**$\mathbf{H_2}$$CO_2^-$ ● free ^-O_2C**C**$\mathbf{H_2}$**C**$\mathbf{H_2}$$CO_2^-$.

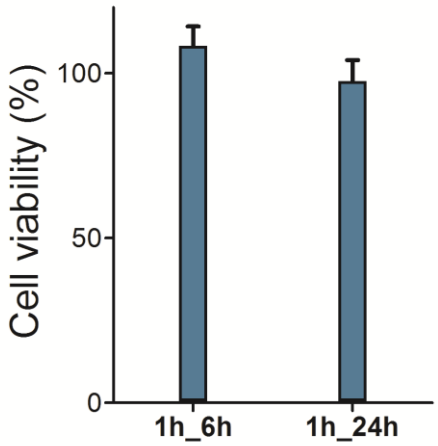

Figure S39. MES toxicity in PC-3 cells. Control experiments performed treating PC-3 cells with MES (2 mM) under light irradiation, using two different incubation conditions. Cells were plated in 96-well plates with a density of 4000 cells per well supplemented with serum and antibiotics and left to grow for 24 h at 37 °C with 5% CO_2 and 90% humidity. MES was then dissolved in the cell culture medium to reach a 2 mM concentration and cells were incubated for 1 h and then irradiated for 1 min with 460-nm light (light dose 0.36 $J \cdot cm^{-2}$). Afterwards, cells were either incubated for other i) 6 hours or ii) 24 h before medium was replaced and cells grown of a total of 48 h. The SRB assay was employed for both incubation conditions to evaluate cell density.

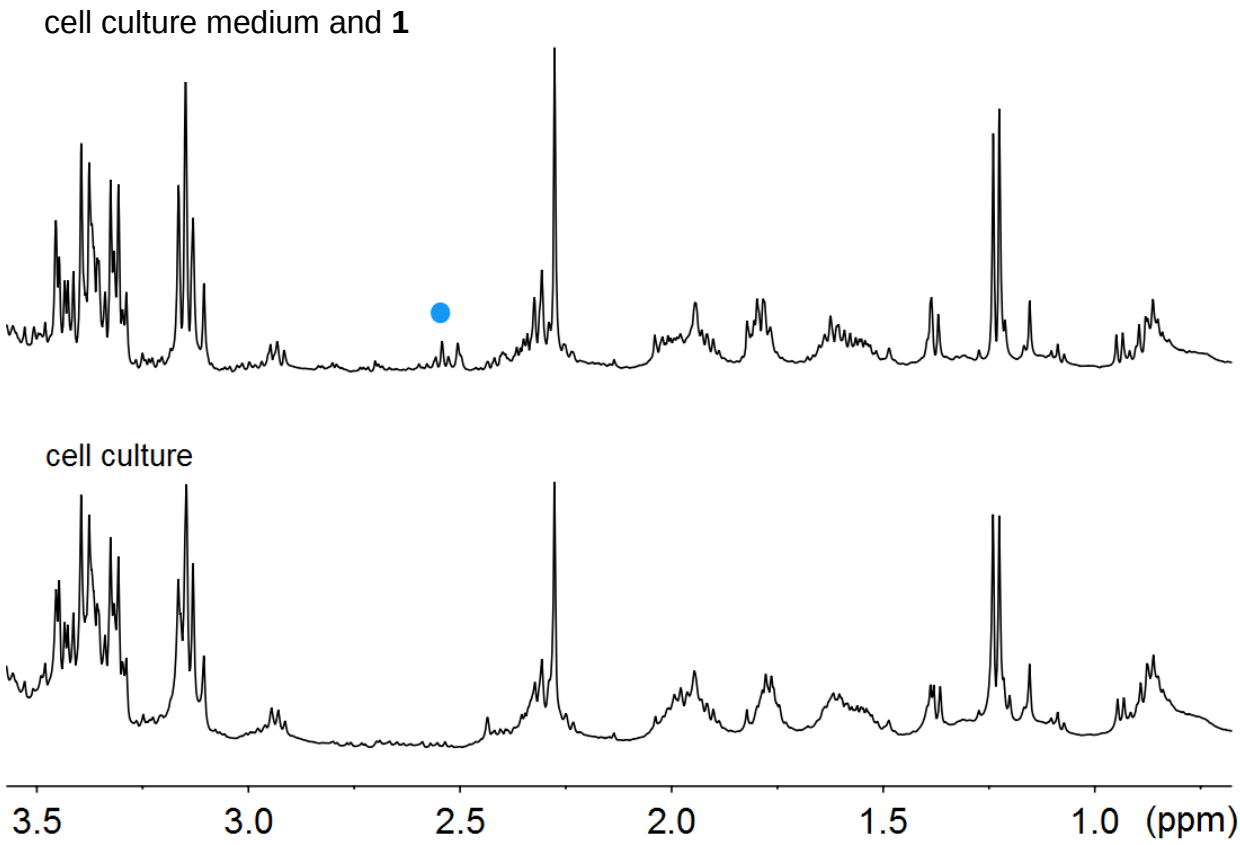

Figure S40. Assessment of the presence of **1** in cell culture medium without MES buffer. ^{1}H NMR spectra of cell culture medium/D_2O (9:1) solution containing 120 µM **1**. Cell culture medium corresponds to Ham's F-12K medium supplemented with 10% fetal bovine serum and 1% penicillin/streptomycin. ^{1}H NMR signal labelling: ● Pt–OCO**CH$_2$**CH$_2$CO$_2^-$.

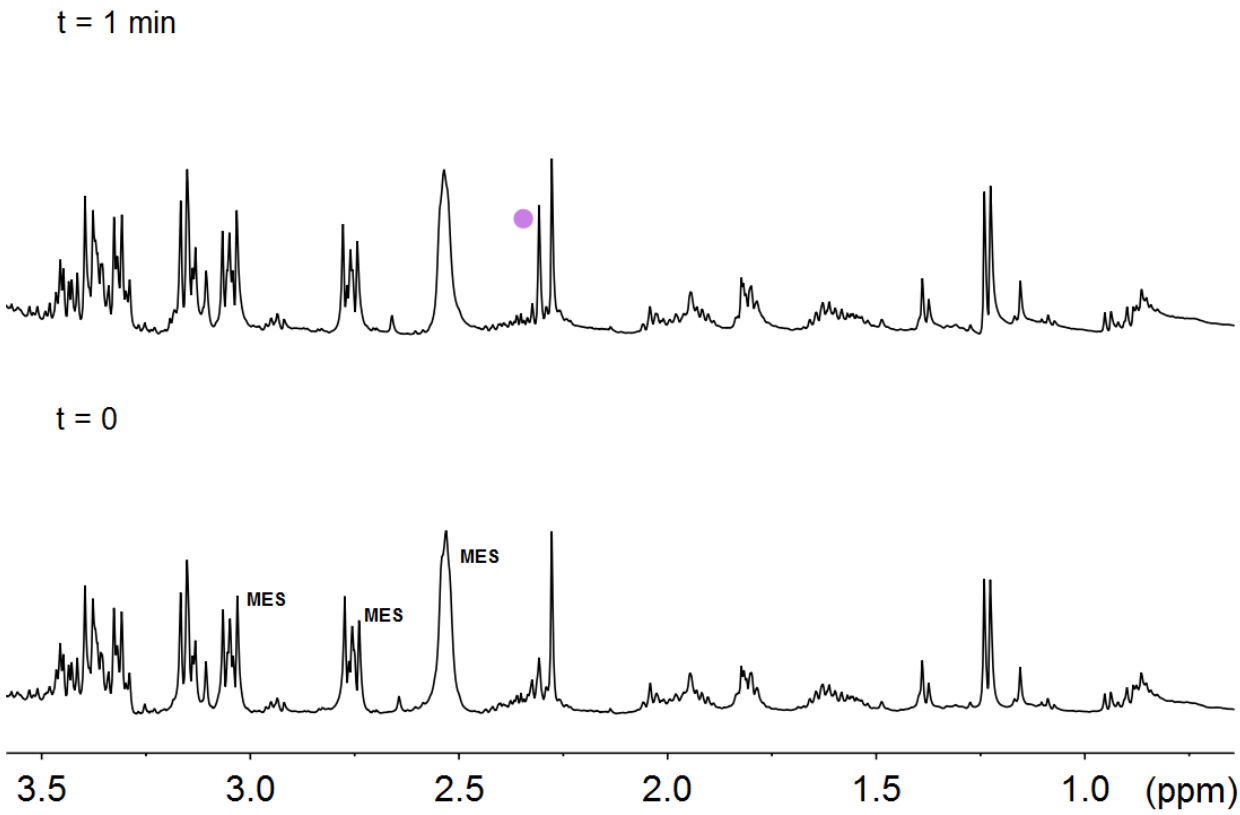

Figure S41. Photolysis of **1** in cell culture medium in the presence of **Rf** and MES. ^{1}H NMR spectra of cell culture medium/MES/D_2O (7.5:1.5:1) solution containing 120 µM **1** and 40 µM **Rf** under 460-nm light irradiation (6 mW·cm^{-2}) for t_{irr} = 0 and 1 min. Cell culture medium corresponds to Ham's F-12K medium supplemented with 10% fetal bovine serum and 1% penicillin/streptomycin. ^{1}H NMR signal labelling: ● free $^{-}O_2C\mathbf{CH_2CH_2}CO_2^{-}$ (compared to Figure S30, the triplet signal of **1** at 2.55 ppm is here buried under one of the MES signals).

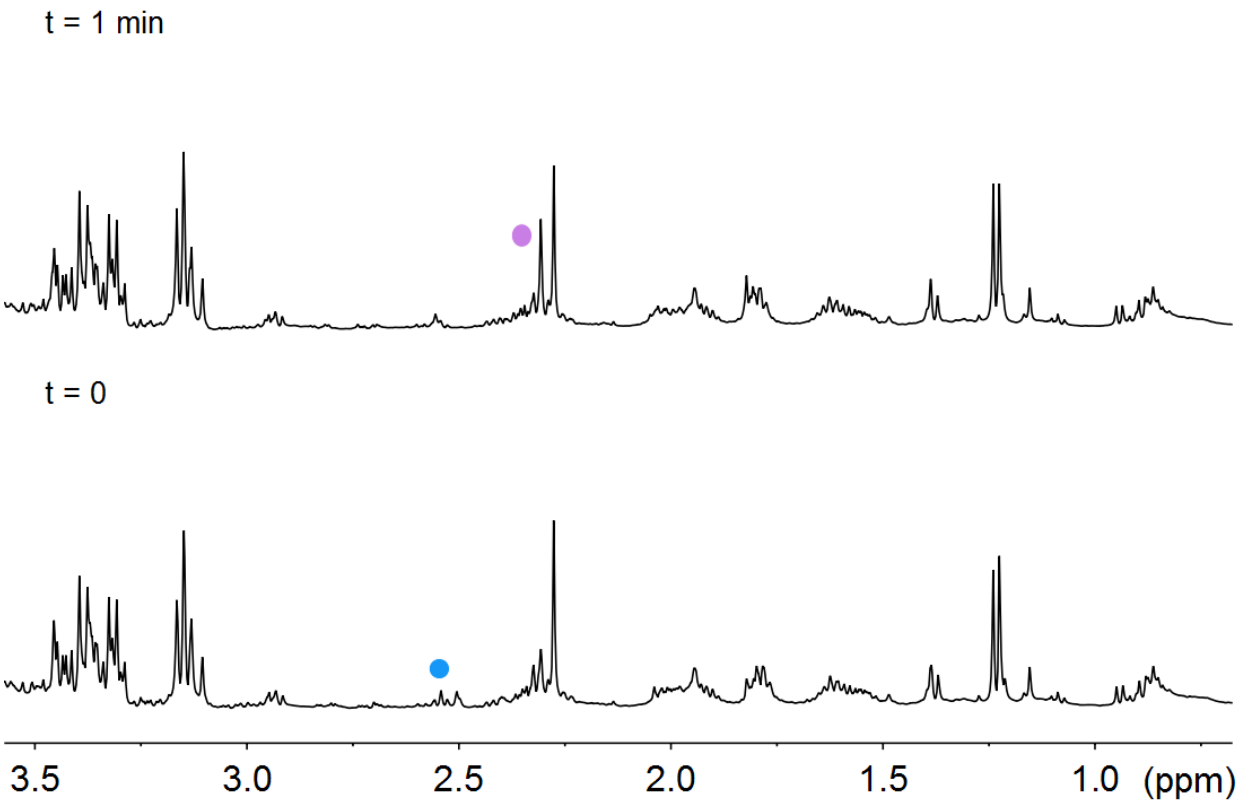

Figure S42. Photolysis of **1** in cell culture medium in the presence of **Rf**. ^{1}H NMR spectra of cell culture medium/H_2O/D_2O (7.5:1.5:1) solution containing 120 μM **1** and 40 μM **Rf** under 460-nm light irradiation (6 mW·cm^{-2}) for t_{irr} = 0 and 1 min. Cell culture medium corresponds to Ham's F-12K medium supplemented with 10% fetal bovine serum and 1% penicillin/streptomycin. ^{1}H NMR signal labelling: ● Pt–OCO**CH$_2$**CH$_2$CO$_2^-$, ● free $^-$O$_2$C**CH$_2$CH$_2$**CO$_2^-$.

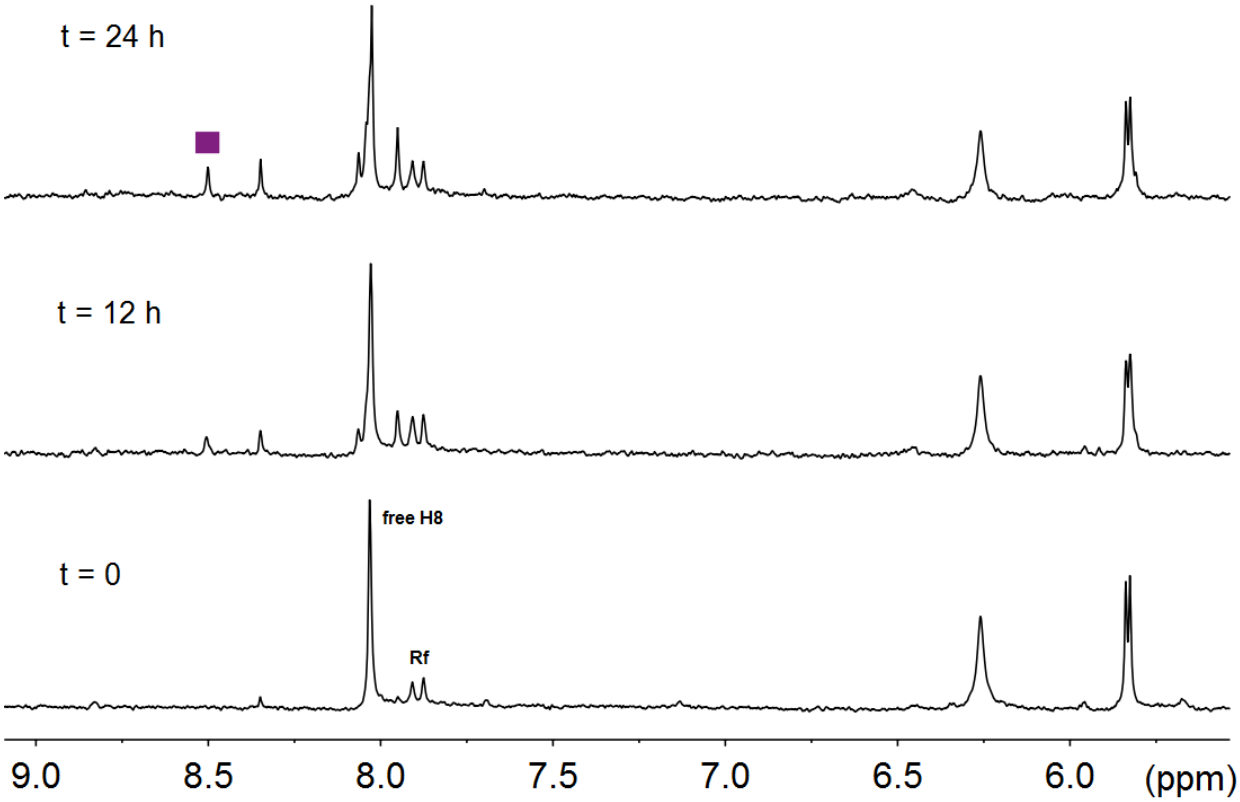

Figure S43. Light-activated platination of 5′-guanosin monophosphate (GMP) by **Rf/1**. ^{1}H NMR spectra of a MES/D_2O (9:1) solution (1.5 mM, pH 6.0) of 120 µM **1**, 50 µM **Rf** after 460-nm light irradiation (1 min, 2.5 mW·cm^{-2}) and incubation with GMP (0.5 mM) for t = 0, 12 and 24 h. ^{1}H NMR signal labelling: : ■ mono-adduct *cis*-$[Pt(NH_3)_2(N7\text{-}GMP)_2]^{2-}$.

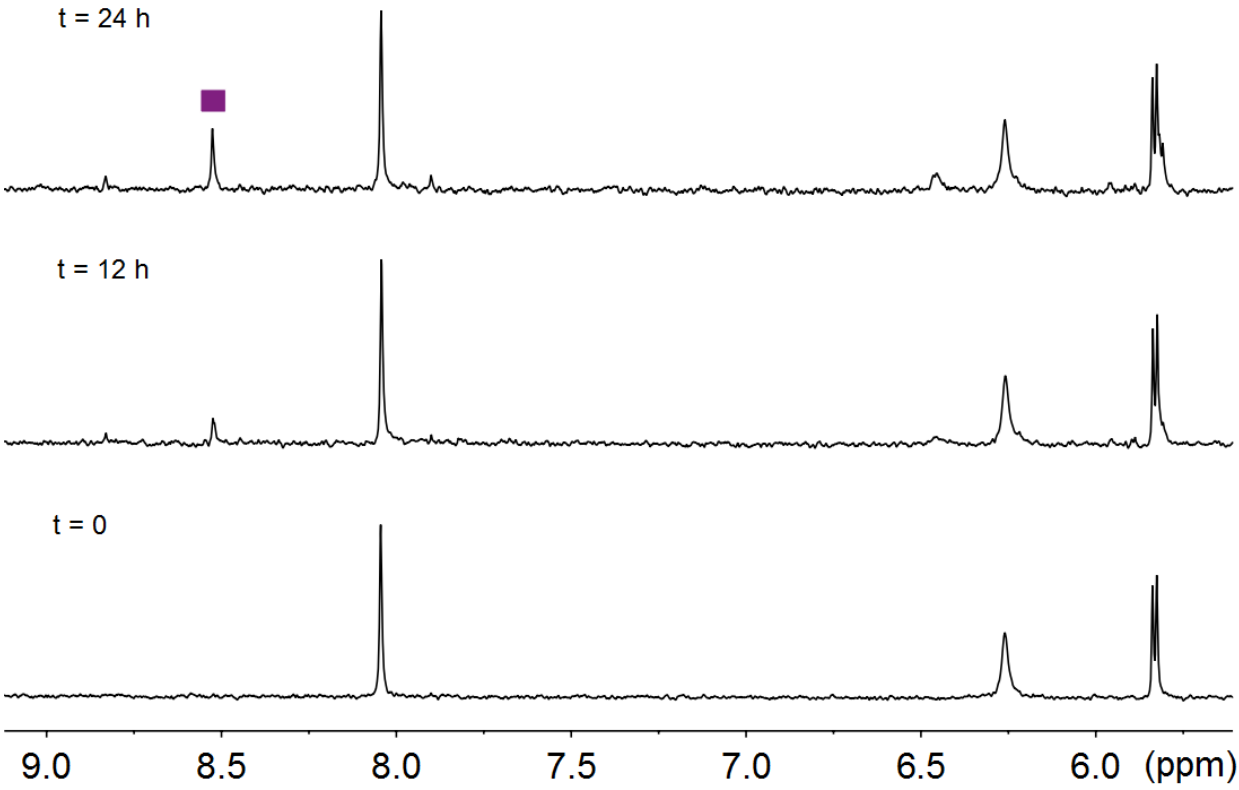

Figure S44. Platination of 5′-guanosin monophosphate (GMP) by cisplatin. ^{1}H NMR spectra of a MES/D_2O (9:1) solution (2 mM, pH 6.0) of 120 µM cisplatin and incubation with GMP (0.5 mM) for t = 0, 12 and 24 h. ^{1}H NMR signal labelling: ■ mono-adduct *cis*-$[Pt(NH_3)_2(N7\text{-}GMP)_2]^{2-}$.

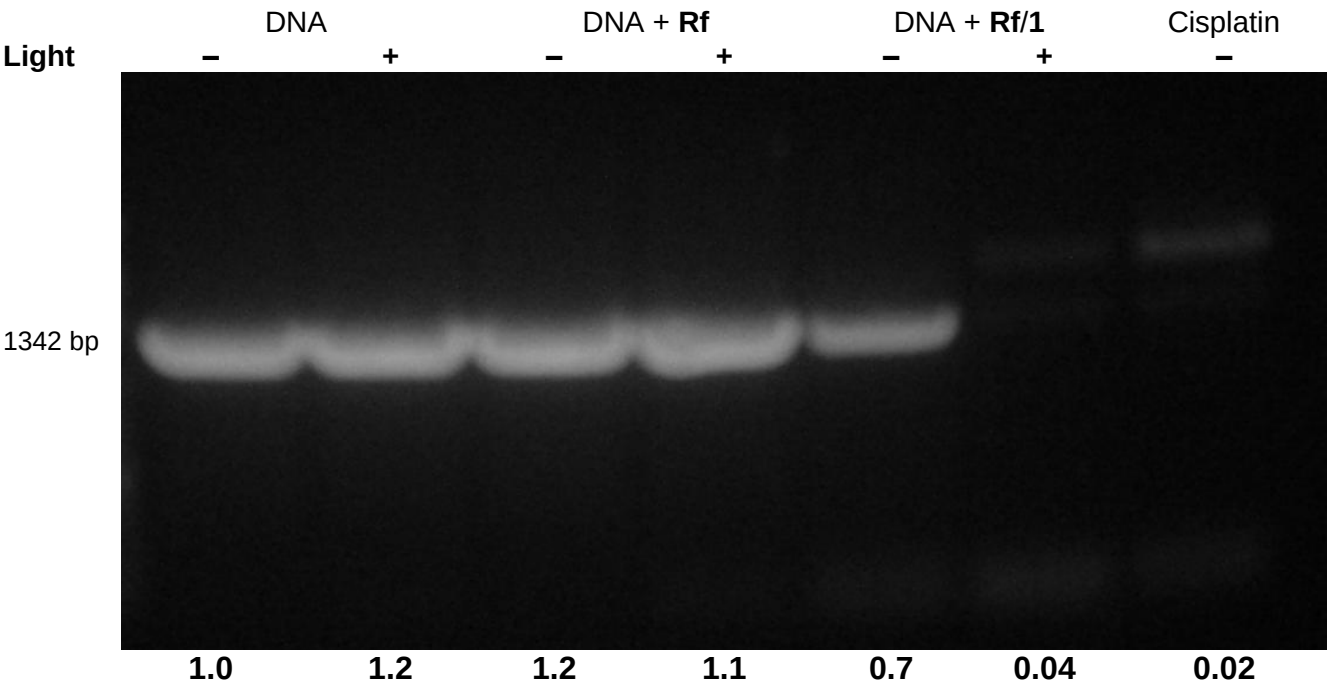

Figure S45. Inhibition of the polymerase chain reaction (PCR) using as template pET28b incubated with **Rf** (2.5 μM), **Rf**/**1** (2.5:10 μM) and cisplatin (10 μM) in the dark and under 30 s of light irradiation at 460 nm (2.5 $mW \cdot cm^{-2}$, 1.5 mM MES and pH 6). Values below the gel indicate intensities of amplified DNA fragment normalized by that of the DNA control in the dark.

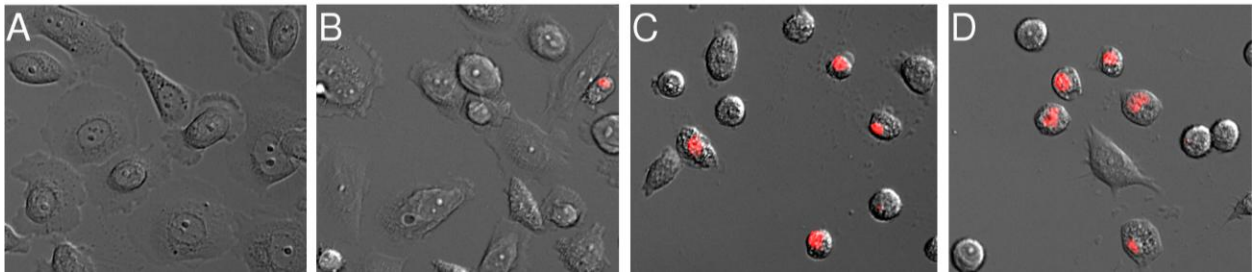

Figure S46. Morphological analysis of PC-3 cells. Merged DIC (Differential Interference Contrast) and fluorescence microscopy images showing the effects of **Rf/1** on PC-3 cells upon light irradiation. (A) untreated PC-3 cells, (B) **Rf/1** (30:120 µM) in the dark, (C) **Rf/1** (30:120 µM) activated by 460-nm light (light dose 0.36 $J \cdot cm^{-2}$) and (D) cisplatin (120 µM) in the dark. All samples were treated in the presence of 2 mM of MES. Cells were stained at the end of the incubation period (48 h) using the dye SYTOX® AADvanced™ (Invitrogen™) for dead cells (red channel).

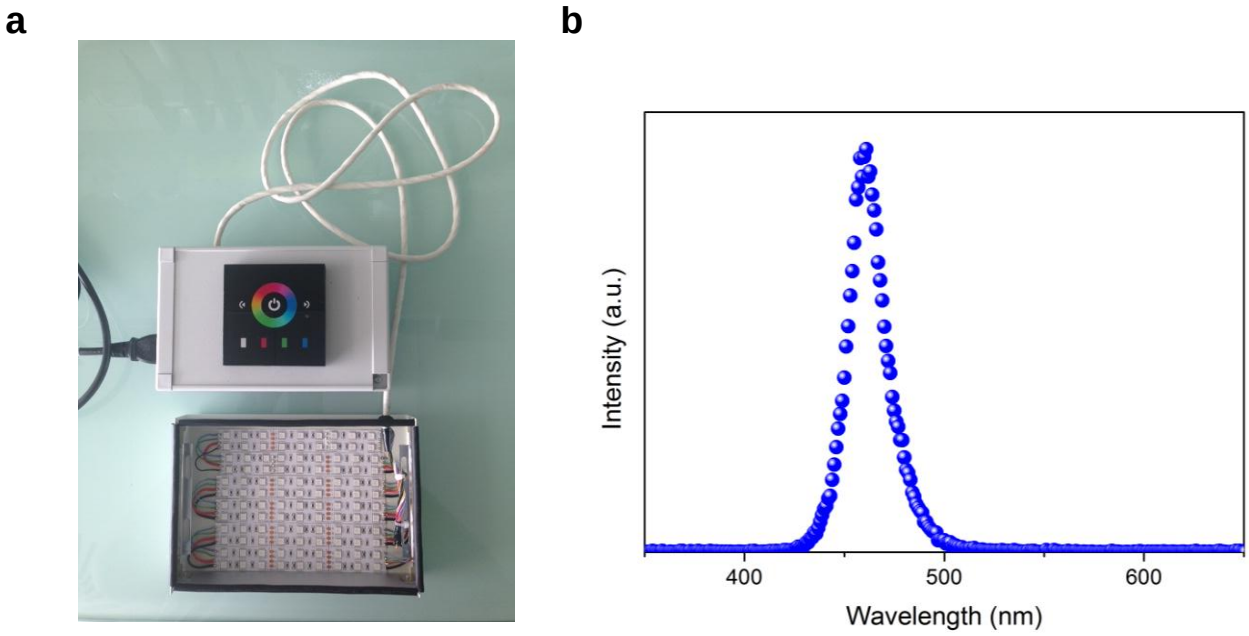

Figure S47. LED setup for cell work and emission profile. (**a**) Custom-made array of blue emitting LEDs used for irradiation of 96-well plates. (**b**) Emission profile of the LED array (460 nm, 6 $mW \cdot cm^{-2}$) employed in the cell work experiment.

Experimental details

Materials

(-)-Riboflavin (**Rf**), formic acid, 2-(N-morpholino)ethanesulfonic acid (MES), sodium phosphate monobasic monohydrate, guanosine 5′-monophosphate disodium salt hydrate (GMP), cisplatin were purchased from Sigma Aldrich, sodium phosphate dibasic from PANREAC and K_2PtCl_4 from Precious Metals Online. All chemicals were used as received without additional purification. Ham's F-12K (Kaighn's) medium nutrient mixture and fetal bovine serum (FBS) were purchased from Invitrogen. Penicillin – Streptomycin was purchased from Teknovas. The pET28b plasmid was purchased from Novagen, DNA primers from Sigma and the Dream Taq polymerase and SYBR Safe dye from Thermo-Fisher.

Synthesis of *cis,cis,trans*-$[Pt(NH_3)_2(Cl)_2(O_2CCH_2CH_2CO_2H)_2]$ (1)

The platinum complex was synthesized by following the procedure described by M. Reithofer et al.[5]

Instrumentation

Nuclear Magnetic Resonance (NMR). ^{1}H NMR spectra of the various samples were recorded on an AVANCE III Bruker 500 NMR spectrometer using standard pulse programs. Chemical shifts were reported in parts-per-million (δ, ppm) and referenced to the residual solvent peak.

UV–Vis absorption spectroscopy (UV-vis). All spectra of **1** and **Rf** were acquired in aqueous solution or buffers using a Varian Cary 5000 spectrophotometer.

Photoirradiation experiments

Photoirradiation experiments were performed on aqueous and buffer solutions obtained dissolving **1** and **Rf** at different concentrations in a 1 mL glass vial and irradiating the whole volume with a LED light source (λ_{irr} = 460 nm, 2.5 mW·cm^{-2}, Prizmatix LED Multi-Wavelength MWLLS-11).

In the case of cell experiments, black 96-well plates were photoirradiated using the blue LED array shown in Figure S37 (λ_{irr} = 460 nm, 6 mW·cm^{-2}). Power densities were measured with a Ophir photonics power meter.

Quantum yield determination by actinometry.

Ferrioxalate actinometry was employed to determine the photon flux of the blue LED array (λ_{irr} = 460 nm, 6 mW·cm^{-2}) and the yield of the photochemical activation for the **Rf**/**1** system. Samples were irradiated in 96-well plates as described in the modified method of Bonnet and co-worker.[3] ^{1}H NMR was employed to quantify the concentration of succinate ligand photoreleased and determine the yield of the photochemical reaction. Actinometry experiments were repeated three times.

Computational details

All calculations were performed with the Gaussian 09 program.[6] The systems were analyzed with Density Functional Theory, using the PBE0/def2-SVP combination, which was previously used in similar studies.[7] Solvent was considered by means of the polarized continuum model (PCM) with water as implicit solvent, and dispersion interactions were taken into account using Grimme's dispersion correction with Becke and Johnson's damping.[8] The geometries were optimized and frequency calculations were run to ensure the lack of imaginary modes. Several isomers were found for each of the complexes presented;

only the global minima are presented in this work. The binding energy was calculated as the electronic energy balance of the reaction **Rf** + **1** → **Rf**/**1**.

Polymerase chain reaction (PCR)-inhibition assay using Rf/1-treated DNA. 2 ng/µL pET28b was light irradiated at 460 nm for 30 s (2.5 $mW \cdot cm^{-2}$) in presence of 2.5 µM of **Rf** and 10 µM of **1** in 1.5 mM MES at pH 6. As negative controls, DNA and DNA incubated with 2.5 µM **Rf** were also irradiated. Moreover, non-irradiated controls were run for each sample. As positive control, DNA was also incubated with 10 µM cisplatin. After incubating irradiated and non-irradiated mixtures for 24 h in the dark, 2 ng of plasmid DNA were used as template for the amplification of 1342 bps fragment by using the following primers: AACTTAATGGGCCCGCTAACAG (primer forward) and CGTCCCATTCGCCATCC (primer reverse). PCR was performed using the Dream Taq polymerase according to the manufacturer´s protocol. PCR was run for 30 cycles and its products were analysed by DNA electrophoresis using 1% agarose gels and SYBR Safe as dye to visualize DNA. The DNA bands were quantified using Image J.

Photocatalysis kinetic model

Assuming the reaction scheme reported below in which **Rf** acts as a photocatalyst, we have adopted a simplified kinetic model in which the reaction rate depends on both **1** and **MES** Eq. (1) (Figure S10 and S11). Nevertheless, such rate can be approximated with as a pseudo-first order reaction considering that the initial concentration of MES is much larger than the initial concentration of **1**. Thus, the concentration of MES remains constant during the chemical reaction. Within this approach, a pseudo-first order reaction constant (k_{obs} = 10.0 ± 0.1·10^{-3} s^{-1}) can be calculated fitting experimental data to Eq (2) (Figure S12) or to Eq (3) (Figure S10). Moreover, a second order reaction constant (k = 1.3 ± 0.1 $M^{-1}s^{-1}$) can be calculated using Eq (4) by fitting the experimental data for k_{obs} at different $[MES]_o$ (Figure S13).

Reaction scheme

$2[MES] + [\mathbf{Rf}] \rightarrow 2[MES^{\bullet+}] + [\mathbf{Rf}H_2/\mathbf{Rf}H^-]$

$[\mathbf{Rf}H_2/\mathbf{Rf}H^-] + [\mathbf{1}] \rightarrow [\mathbf{Rf}] + [Pt^{II}]$

$2[MES] + [\mathbf{1}] \rightarrow 2[MES^{\bullet+}] + [Pt^{II}]$

Kinetic Model

$\text{rate}(v) = k[MES][\mathbf{1}]$ (1)

$[\mathbf{1}] = [\mathbf{1}]_0 e^{-k_{obs}t}$ (2)

$v = k_{obs}[\mathbf{1}]$ $\quad [MES]_o >> [\mathbf{1}]_o$ (3)

$k_{obs} = k[MES]_o$ (4)

References

1. Adamo, C. & Barone, V. Toward reliable density functional methods without adjustable parameters: The PBE0 model. *J. Chem. Phys.* **110,** 6158–6170 (1999).

2. Weigend, F. & Ahlrichs, R. Balanced basis sets of split valence, triple zeta valence and quadruple zeta valence quality for H to Rn: Design and assessment of accuracy. *Phys. Chem. Chem. Phys.* **7**, 3297–3305 (2005).

3. Hopkins, S. L. *et al.* An in vitro cell irradiation protocol for testing photopharmaceuticals and the effect of blue, green, and red light on human cancer cell lines. *Photochem. Photobiol. Sci.* **15**, 644–653 (2016).

4. Demas, J. N., Bowman, W. D., Zalewski, E. F. & Velapoldi, R. A. Determination of the quantum yield of the ferrioxalate actinometer with electrically calibrated radiometers. *J. Phys. Chem.* **85**, 2766–2771 (1981).

5. Reithofer, M., Galanski, M., Roller, A. & Keppler, B. K. An Entry to Novel Platinum Complexes: Carboxylation of Dihydroxoplatinum(IV) Complexes with Succinic Anhydride and Subsequent Derivatization. *Eur. J. Inorg. Chem.*, 2612–2617 (2006).

6. Frisch, M. J. *et al. Gaussian 09*. (Gaussian, Inc., 2009).

7. Infante, I. *et al.* Quantum Dot Photoactivation of Pt(IV) Anticancer Agents: Evidence of an Electron Transfer Mechanism Driven by Electronic Coupling. *J. Phys. Chem. C* **118**, 8712–8721 (2014).

8. Grimme, S., Ehrlich, S. & Goerigk, L. Effect of the damping function in dispersion corrected density functional theory. *J. Comput. Chem.* **32**, 1456–1465 (2011).